A PFAS-steroid axis is associated with lipid and bile acid metabolism in MASLD

Short title: PFAS-steroid axis in MASLD metabolism

Pauli Tikka[1], Aidan McGlinchey[2], Sami F. Qadri[3,4], Ilia Evstafev[1], Alex M. Dickens[1,5], Hannele Yki-Järvinen[3,4], Tuulia Hyötyläinen[6], Matej Orešič[1,2,7,*]

[1]Turku Bioscience Centre, University of Turku and Åbo Akademi University, FI-20520 Turku, Finland

[2]School of Medical Sciences, Faculty of Medicine and Health, Örebro University, SE-702 81 Örebro, Sweden

[3]Department of Medicine, University of Helsinki and Helsinki University Hospital, Helsinki, Finland

[4]Minerva Foundation Institute for Medical Research, Helsinki, Finland

[5]Department of Chemistry, University of Turku, FI-20014 Turku, Finland

[6]School of Science and Technology, Örebro University, SE-702 81 Örebro, Sweden

[7]Department of Life Technologies, University of Turku, FI-20014 Turku, Finland

*Corresponding author

Professor Matej Orešič, PhD

Turku Bioscience Centre, University of Turku and Åbo Akademi University, FI-20520 Turku, Finland

Phone: +358 44 9726094; Email: matej.oresic@utu.fi

Keywords: bile acids; endocrine disruption; lipid metabolism; MASLD; PFAS; steroid hormones.

Declaration of interest: The authors declare that no competing interests exist.

Financial support statement: This study was supported by the "Investigation of endocrine-disrupting chemicals as contributors to progression of metabolic dysfunction-associated steatotic liver disease" (EDC-MASLD) consortium funded by the Horizon Europe Program of the European Union under Grant Agreement 101136259 (to T.H. and M.O.), the Novo Nordisk Foundation (grant no. NNF20OC0063971 to T.H. and M.O.), Academy of Finland (grant no. 333981 to M.O. and no. 309263 to H.Y.-J.), Swedish Research Council (grant no. 2016-05176 to T.H and M.O), Juselius Foundation (to H.Y.-J.), the EPoS (Elucidating Pathways of Steatohepatitis) project funded by the Horizon 2020 Framework Program of the European Union (grant no. 634413, to M.O., H.Y.-J., and T.H.), the Swedish Knowledge Foundation (grant no. 20220122, to T.H. and M.O.), the Orion Research Foundation (to S.F.Q.), the Yrjö Jahnsson Foundation (20207313 to S.F.Q.), the Maud Kuistila Memorial Foundation (2021-

0301B to S.F.Q.), the Emil Aaltonen Foundation (210182 to S.F.Q.), the Finnish Medical Foundation (5843 to S.F.Q.), and the Biomedicum Helsinki Foundation (20230241 to S.F.Q.). The authors would also like to thank the Turku Metabolomics Centre and Biocentre Finland for funding the instruments at the University of Turku used in this manuscript. Views and opinions expressed are those of the authors only and do not necessarily reflect those of the European Union. Neither the European Union nor the granting authority can be held responsible for them.

Authors contributions: Conceptualization and design of study (MO, HYJ, TH), clinical study (SFQ, coordinated by HYJ), metabolomics analysis (IE, AMD, TH), data analysis and interpretation (PT, with critical input from SFQ, AM, HYJ, TH, supervised by MO), manuscript preparation (PT, MO, TH), critical review and editing (all authors).

Data availability statement: Data from the clinical study are available upon request and an appropriate institutional collaboration agreement.

Abbreviations: Bile acids; BPA, bisphenol A; CA, cholic acid; CErs, ceramides; CYP7A1, cholesterol 7a-hydroxylase; DCA, deoxycholic acid; DG, diacylglycerol; EC, environmental contaminants; EDCs, endocrine-disrupting chemicals; GCA, glycocholic acid; GCDCA, glycochenodeoxycholic acid; HCA, hyocholic acid; HDCA, hyodeoxycholic acid; HexCers, hexosylceramides; HOMA-IR, homeostatic model assessment of insulin resistance; hPPARa, humanized PPARa; IR, insulin resistance; LCA, lithocholic acid; LPCs, lysophosphatidylcholines; LPEs, lysophosphatidylethanolamines; MASLD, metabolic-dysfunction associated steatotic liver disease; MASH, metabolic-dysfunction associated steatohepatitis; PCs, phosphatidylcholines; PEs, phosphatidylethanolamines; PFAS, perfluorinated alkyl substances; PFHxS, perfluorohexanesulfonic acid; PFNA, perfluorononanoic acid; PFOA, perfluorooctanoic acid; PFOS, perfluorooctanesulfonic acid; SMs, sphingomyelins; TCA, taurocholic acid; TCDCA, taurochenodeoxycholic acid; TG, triacylglycerol. 11-Ketotestosterone (11-KT), 11b-OH-Androstenedione (11b-OHA4), 11-Ketodihydrotestosterone (11-KDHT), 11-Ketoandrostenedione (11-KA4), Dehydroepiandrosterone (DHEA), Testosterone / (&) Epi-testosterone (T/Epi-T), Androsterone (AN), Dihydrotestosterone (DHT), Androstenedione (A4), Estradiol (E2), Estrone (E1), Cortisone (E), 11-Deoxycortisol (S), Corticosterone (B), Aldosterone (A), 17a-OH-Pregnenolone (17a-OHP5), 17a-OH-Progesterone (17a-OHP4), 11-Deoxycorticosterone (DOC), Pregnenolone (P5), Progesterone (P4). Androgenes (A), Estrogens €, Glucocorticosteroids (G), mineralcorticosteroids (M) and Progesterones (P).

Abstract

Background & Aims: Per- and polyfluoroalkyl substances (PFAS) are persistent endocrine-disrupting chemicals associated with metabolic dysfunction, including metabolic dysfunction-associated steatotic liver disease (MASLD). While PFAS perturb lipid and bile acid (BA) metabolism in a sex-specific manner, the underlying mechanisms remain unclear. We tested whether steroid hormones mediate PFAS-associated metabolic alterations.

Methods: In 104 patients with biopsy-characterized MASLD, we performed sex-stratified analyses applied liquid chromatography coupled to mass spectrometry (LC-MS) for chemical analysis, integrating circulating steroids, PFAS exposure, hepatic lipidomics and BA profiles.

Results: Steroid hormones were associated with MASLD severity in a sexually-dimorphic manner. Dihydrotestosterone showed consistent inverse associations with steatosis, fibrosis, necroinflammation and insulin resistance, particularly in females. PFAS exposure was associated with altered steroid profiles, predominantly indicating suppressed steroidogenesis in females. These PFAS-associated hormonal changes were linked to downstream alterations in hepatic lipids and BAs. Mediation analysis supported indirect effects of PFAS on metabolic pathways *via* steroids, including testosterone/epi-testosterone-mediated effects on ether phospholipids and estradiol-mediated effects on lithocholic acid. Females exhibited stronger PFAS-steroid-BA associations, whereas males showed weaker, lipid-centric effects.

Conclusions: PFAS exposure is associated with sex-specific disruption of steroid hormone pathways that may link environmental exposure to lipid and BA dysregulation in MASLD. These findings identify steroid hormones as potential key mediators of PFAS-associated metabolic dysfunction and highlight sex as a critical determinant in environmental liver disease.

Introduction

Metabolic dysfunction-associated steatotic liver disease (MASLD) affects ~30% of the global population and is characterized by hepatic lipid accumulation, insulin resistance, and progressive liver injury (Younossi et al. 2023). While obesity and metabolic syndrome are key drivers, environmental factors, particularly endocrine-disrupting chemicals (EDCs), are increasingly implicated in disease initiation and progression (Deierlein et al. 2017; Foulds et al. 2017; Giulivo et al. 2016; Heindel et al. 2017). EDCs can perturb endocrine signaling and metabolic pathways, acting either as early triggers or as accelerators of disease progression toward steatohepatitis and fibrosis (Treviño and Katz 2018; Vujkovic et al. 2022; Wahlang et al. 2019).

Per- and polyfluoroalkyl substances (PFAS) are ubiquitous, persistent EDCs associated with dysregulated lipid metabolism, bile acid (BA) homeostasis, and liver injury (Zhang et al. 2024). We previously demonstrated sex-specific metabolic effects of PFAS in MASLD, with stronger and predominantly adverse associations in females, including altered lipid and BA profiles (Sen et al. 2022). However, the mechanisms underlying this sexual dimorphism remain unresolved.

Steroid hormones are central regulators of hepatic metabolism, modulating lipid homeostasis,

insulin sensitivity, and inflammation (Ortiz-Huidobro et al. 2021; Shen and Shi 2015; Song and Choi 2022; Yang et al. 2021). Glucocorticoids promote lipid accumulation and insulin resistance (Polyzos and Targher 2024), whereas estrogens generally exert protective metabolic effects (Yang et al. 2014). Androgens exhibit context-dependent and sex-specific actions, contributing to divergent metabolic phenotypes in males and females. Experimental and epidemiological evidence indicates that PFAS can disrupt steroidogenesis and hormone signaling (Cui et al. 2020; Joensen et al. 2013; Kang et al. 2016; Wang et al. 2021; Zhou et al. 2017), but whether these alterations associate with PFAS-linked metabolic dysfunction is unknown.

Here, we investigated steroid hormones as potential mediators of PFAS effects in MASLD. We examined (i) associations between steroids and disease severity, (ii) relationships between PFAS exposure and steroid profiles, and (iii) whether steroid alterations link PFAS exposure to changes in hepatic lipid and BA metabolism. By integrating clinical, metabolomic, and mediation analyses, we aimed to define potential key endocrine mechanisms underlying sex-specific environmental effects in MASLD.

Methods

Clinical cohort

The study population has been described previously (Sen et al. 2022). Briefly, 104 patients (69 females, 35 males) undergoing laparoscopic bariatric surgery were included (**Table 1**).

Inclusion criteria were: (i) age 18–75 years; (ii) absence of acute or chronic diseases other than obesity, type 2 diabetes or hypertension; (iii) alcohol consumption <20 g/day (women) or <30 g/day (men); (iv) no evidence of other liver diseases or inborn metabolic disorders; and (v) no exposure to hepatotoxic drugs. Elevated liver enzymes were not an exclusion criteria. Clinical measurements were performed as described previously (Luukkonen et al. 2016). Demographic characteristics of the study population is shown in **Table S1**. Cases were defined as steatosis, fibrosis, or necroinflammation >0, and HOMA-IR >1.5, with corresponding controls defined as ≤0 or ≤1.5, respectively (Sen et al. 2022).

This is a cross-sectional observational study; therefore, causal inference cannot be established.

The study protocol was approved by the Ethical Review Committee of the Hospital District of Helsinki and Uusimaa (284/13/03/01/13). The study was conducted in accordance with the Declaration of Helsinki. Each participant provided written informed consent after being explained the nature and potential risks of the study.

Steroid analysis

The steroids were extracted using a liquid-liquid extraction method. 20 µL of internal standards (**Table S2**) solution was added to 100 µL of each serum sample and extracted with with tert-butyl methyl ether. The samples were vortex mixed for 10 minutes and the upper layer was collected, evaporated to under nitrogen flow at 40°C and reconstituted in 50 µL of solvent (acetonitrile:water, 3:7, v/v). Matrix quality control samples were prepared from the pooled serum sample using the same preparation procedure as the test samples. Blanks were prepared in a similar manner, but with saline instead of serum. The extracts were then stored

at −80 °C until analysis.

Calibration curves contained 11-Deoxycorticosterone (DOC), 11b-OH-Androstenedione (11b-OHA4), 11-Deoxycortisol (S), 11-Ketodihydrotestosterone (11-KDHT), 11-Ketotestosterone (11-KT), 17a-OH-Pregnenolone(17a-OHP5), 17a-OH-Progesterone(17aOH-P4), 11-Ketoandrostenedione (11-KA4), Aldosterone (A), Androstenedione (A4), Androsterone (AN), Corticosterone (B), Cortisol (F), Cortisone (E), Dehydroepiandrosterone (DHEA), Dihydrotestosterone (DHT), Estradiol (E2), Estrone (E1), Pregnenolone (P5), Progesterone (P4), Testosterone / Epi-testosterone (T/Epi-T) were prepared by mixing 20 µL of solvent (acetonitrile:water, 3:7, v/v), 40 µL of internal standard solution and 40 µL of corresponding working solution (**Table S3**). The final calibration curve levels were corresponding to the following concentration levels in serum: 5.00, 10.0, 20.0, 50.0, 100, 200, 500, 1000, 2000, 10000, 20000, 50000, 100000, 200000 pM. To control the calculated concentration during the analytical run, solvent control samples were prepared. The working solution with a concentration corresponding of 10000 pM in serum was prepared utilizing the procedure for preparing the calibration curve.

The samples were analyzed using ultra-high-performance liquid chromatography tandem mass spectrometry method (UHPLC-MS/MS) (**Table S4).** Briefly, the UHPLC system used in this work was an ExionLC system from AB Sciex LLC (Framingham, MA, USA). The system was equipped with an autosampler (maintained at 10 °C), two pumps and a column thermostat (maintained at 35 °C; **Table S5**). Separations were performed on a Kinetex Biphenyl 100 Å (2.1 mm × 100 mm, particle size 1.7 µm) by Phenomenex (Torrance, CA, USA). The mass spectrometer coupled to the UHPLC was a SCIEX Triple Quad™ 7500 instrument from AB Sciex LLC interfaced with OptiFlow Pro ion source (ESI) ion source. Analyses were performed in both negative and positive ion modes and Sciex OS (SCIEX OS 3.0.0.3339) was used for all data acquisition. Quality control was performed throughout the run with use of solvent control samples, matrix control samples and blanks.

Metabolomic and PFAS analyses

Hepatic lipidomics and metabolite profiling were performed as described previously (Luukkonen et al. 2016; Sen et al. 2022), including lipidomics, polar and semi-polar metabolites, and targeted bile acid analysis. PFAS concentrations were measured from serum samples as described by Sen et al. (Sen et al. 2022). Combined summary datasets are provided in **Tables S6–S7**.

Statistical analyses

Data were log2-transformed and autoscaled to zero mean and unit variance prior to further analysis. Associations were assessed using Spearman correlations and linear models, adjusted for age, BMI, and sex where appropriate. Chord plots were constructed using non-rejection rate (NRR) thresholds (0.2 overall; lower thresholds for sex-stratified analyses; **Figs. S1–S2**). The levels of high vs. low HOMA-IR levels (case vs. control) were chosen to be above or below 1.5, respectively (Sen et al. 2022). The other cases (steatosis, fibrosis, necroinflammation) were defined as those having values above 0.

Causal mediation analysis

Causal mediation analysis (CMA) was performed using the R package *mediation* (Kurz 2023) to assess whether steroid hormones mediate associations between PFAS and lipid or bile acid outcomes. Models included (i) a mediator model (M) linking PFAS to steroids, and (ii) an outcome model (Y) linking PFAS and steroids to metabolic outcomes.

All models were adjusted for age, BMI, and sex (Walker 2024). The following quantities were estimated: average causal mediation effect (ACME; indirect effect), average direct effect (ADE), total effect, and proportion mediated. Analyses were performed using 100 simulations with default parameters using the *mediation* package.

Results

Steroid hormones showed large biological variation

Steroid concentrations showed inter-individual variability spanning several orders of magnitude (**Table S6**). Cortisone was the most abundant steroid in both sexes, followed by dehydroepiandrosterone and 11β-hydroxyandrostenedione. In males, testosterone/epitestosterone was among the most abundant steroids.

The cohort was characterized by severe obesity (mean BMI >47), a predominance of females (66%), and an age range of 29–67 years. Notably, 68% of females were below the median menopausal age in Finland.

Steroids are associated with the staging of MASLD

We next investigated associations between steroid hormones and steatosis grade, fibrosis stage, necroinflammation, and HOMA-IR, both in the full cohort and in sex-stratified analyses, considering both case–control comparisons and continuous disease stages (**Figs. 1**, **S3–S9**).

At the case–control level, steroid alterations were more pronounced in females than in males, particularly for steatosis (**Fig. 1A**). In the overall cohort, several steroids were lower in steatotic subjects (**Fig. S3**), including 11-deoxycortisol, pregnenolone, and progesterone. Pregnenolone and progesterone were also reduced in fibrosis, and progesterone was lower in necroinflammation. Subjects with fibrosis also showed reduced DHT levels.

In sex-stratified analyses, a broader pattern was observed in females, with eight steroids lower in steatosis (**Fig. S4**), including 11-ketoandrostenedione, 11β-hydroxyandrostenedione, DHT, aldosterone, 11-deoxycorticosterone, 17α-OH-progesterone, pregnenolone, and progesterone. In males, only 11-deoxycorticosterone and pregnenolone were significantly lower (**Fig. S5**). Similar patterns were observed across fibrosis, necroinflammation, and HOMA-IR (**Figs. S3–S5**).

Across continuous disease stages (**Figs. S6–S9**), DHT showed consistent negative associations with steatosis grade, fibrosis stage, necroinflammation, and HOMA-IR in the overall cohort. These associations were primarily driven by females, as DHT was significantly associated with these outcomes only in females in sex-stratified analyses.

Additional associations were observed for multiple steroids. Steatosis grade was negatively associated with 11-deoxycorticosterone, 11β-hydroxyandrostenedione, pregnenolone, and progesterone. Fibrosis stage was associated with testosterone/epitestosterone, while necroinflammation showed associations with androsterone, 11-deoxycortisol, corticosterone, pregnenolone, and progesterone. These patterns were generally consistent across sexes, although not all reached statistical significance in each subgroup.

HOMA-IR showed positive associations with 11β-hydroxyandrostenedione and 11-deoxycortisol in the overall cohort, and additionally with 11-ketotestosterone, 11-ketoandrostenedione, 11-deoxycortisol, and cortisone in males. Overall, androgens showed more associations with clinical parameters in males, predominantly negative, except for positive associations of 11-ketotestosterone and 11-ketoandrostenedione with HOMA-IR.

Age was negatively associated with several steroids (androstenedione, androsterone, dehydroepiandrosterone, estradiol, and progesterone) in the overall cohort, while 11β-hydroxyandrostenedione showed positive associations (**Figs. S10–S11**). Most of these associations were driven by females, except for dehydroepiandrosterone, which showed negative associations only in males. In males, androstenedione, estradiol, and progesterone were not associated with age.

BMI was associated with several steroids only in males, with positive associations observed for estradiol, estrone, androstenedione, and 11-ketotestosterone, and negative associations for androsterone and DHT.

PFAS are associated with disease stage and steroid profiles in sex specific manner

We next examined associations between PFAS (**Table 7**), steroid hormones, and disease stage. PFAS exposure was associated with steroid profiles in a sex-specific manner (**Fig. 2**), with predominantly negative associations between PFAS and steroids. PFAS were also positively associated with HOMA-IR and age, particularly in females. Several steroids, including cortisone, corticosterone, aldosterone, 17α-OH-progesterone, and pregnenolone, were associated with multiple PFAS in the overall cohort.

PFHpA showed the strongest associations, with negative relationships to seven steroids, particularly progestogens, and these effects were most pronounced in females. PFNA and PFOS showed similar but weaker patterns, while PFOA showed a negative association with aldosterone.

PFHxS exhibited negative associations with several steroids in females (including 11-ketotestosterone, cortisone, and corticosterone), whereas in males it showed an opposite trend with positive associations for progestogens (17α-OH-progesterone and progesterone). In contrast, PFHxA showed predominantly positive associations with steroids, particularly dehydroepiandrosterone.

Steroids are associated with bile acids and lipids

We next investigated associations between steroids and bile acids and lipids (**Table S7**). Steroid–metabolite associations showed clear sex-specific patterns (**Fig. 3**, **Fig. S12**).

When analyzing the data from both males and females simultaneously, steroids showed both positive and negative associations with bile acids and lipids, with positive associations largely driven by females. In females, many bile acids were positively associated with steroids, with the exception of selected estrogens and androgens. In contrast, in males, bile acids showed predominantly negative associations with steroids, particularly with androgens.

Associations between steroids and lipids were more similar across sexes but were generally stronger in males. In males, several steroids, particularly androgens and progestogens, were positively associated with cholesteryl esters, sphingomyelins, and phospholipids (PI, PC_O). Saturated triacylglycerols showed negative associations with androgens in males and with estradiol in females. In females, androgens showed negative associations with ceramides and positive associations with phospholipids (LPC, PC_O) and triacylglycerol groups (TG_SFA, TG_MUFA, TG_PUFA).

Network-level analysis (**Fig. 4**) revealed strong interconnections between PFAS, steroids, clinical variables, lipids, and bile acids. PFAS were closely linked to age and sex, and to several steroids. Lipid classes, particularly ceramides and diacylglycerols, showed correlations with both steroids and bile acids. Further analysis using network visualization (**Fig. S13**) showed that lipids clustered more closely with steroids, whereas bile acids formed a more distinct group with weaker direct associations with steroids.

Impacts of PFAS exposure on lipid metabolism may be mediated through steroids and bile acids

To assess whether steroid hormones may link PFAS exposure to metabolic outcomes, we performed causal mediation analysis (CMA). Indirect and direct effects for all subjects are shown in **Fig. 5** and **Table S8**. **Fig. 5A** illustrates the conceptual framework, including average causal mediation effects (ACME) and average direct effects (ADE), while **Fig. 5B** summarizes mediation pathways across all subjects.

Potential steroid-mediated effects of PFAS on lipid and bile acid outcomes were suggested, with testosterone/epitestosterone (T/Epi-T) showing the most pronounced mediation effects (**Fig. 5B**). Sex-stratified analyses (**Figs. S14A–B**; **Tables S9–S10**) identified different dominant mediation effects: in females, dehydroepiandrosterone (DHEA) and 17α-OH-pregnenolone were the primary mediators, whereas in males 11-ketotestosterone and pregnenolone were most prominent. These sex-specific mediation patterns were not altered after adjustment for age and BMI (**Fig. S15**).

Discussion

Steroid hormones are central regulators of hepatic lipid metabolism, insulin sensitivity and inflammation (Dobre et al. 2025; MacMillan et al. 2024; Quagliarini et al. 2023). In this study, we find that a sex-dependent network may link steroid hormones to metabolic dysfunction-associated steatotic liver disease (MASLD) severity, PFAS exposure, and downstream lipid and bile acid (BA) metabolism (Henriksen et al. 2016; India-Aldana et al. 2023; Lee et al. 2011; Seidemann et al. 2024).

Importantly, this study extends prior PFAS research by demonstrating that steroid hormones are not only associated with PFAS exposure but may act as intermediate links between PFAS and hepatic metabolic alterations. While previous studies have reported associations between PFAS and lipid metabolism or hormone levels separately (India-Aldana et al. 2023; Sen et al. 2022), our integrative analyses suggest a connected PFAS–steroid–metabolism axis in MASLD.

DHT) showed the most consistent associations, particularly in females, across steatosis, fibrosis, necroinflammation and insulin resistance. DHT enhances insulin sensitivity and glucose uptake (Frank et al. 2019; Mårin 1995; Saad et al. 2001), yet its metabolic effects are context- and sex-dependent. Elevated androgen activity in females has been linked to insulin resistance and adverse metabolic phenotypes (Münzker et al. 2015; Münzker et al. 2017). This divergence is supported by experimental models showing opposing androgen effects on hepatic metabolism between sexes (Cherubini et al. 2024; Lin et al. 2008).

Dehydroepiandrosterone (DHEA) further highlighted sex-specific metabolic patterns. In males, DHEA was associated with cholesteryl esters and sphingomyelins—lipid classes implicated in MASLD progression (Ramos-Molina et al. 2024; Syed-Abdul 2023). In females, DHEA was instead associated with secondary BAs, suggesting involvement of gut microbiota in steroid metabolism. Microbial regulation of steroid conversion, including androgen metabolism, supports the presence of a gut–liver–steroid axis (Mayneris-Perxachs et al. 2020).

Several additional steroids, including progesterone and pregnenolone, were associated with disease severity and metabolic pathways, consistent with their established roles in hepatic lipid metabolism and insulin sensitivity (Yang et al. 2017). Notably, some steroids were linked to lipid and BA profiles independent of direct associations with disease stage, suggesting broader regulatory roles in hepatic metabolism.

PFAS exposure was associated with altered steroid hormone profiles in a sex-dependent manner, in line with previous evidence of PFAS-induced disruption of steroidogenesis (India-Aldana et al. 2023; Kushnir et al. 2024). In females, most associations were negative, including those involving pregnenolone, the precursor of all steroid hormones, suggesting reduced steroidogenic activity. Experimental studies indicate that PFAS can alter steroidogenic enzyme expression and hormone synthesis (Eggert et al. 2019; Tian et al. 2019). In contrast, associations in males were fewer and often directionally-opposite, although this may partly reflect smaller sample size.

While the cross-sectional design precludes causal inference, the integration of mediation analysis with multi-omics profiling supports a model in which steroid hormones may contribute to linking PFAS exposure to downstream metabolic alterations. In females, PFAS-associated steroids were primarily linked to BA metabolism, particularly secondary BAs, whereas in males associations were more lipid-centered. These findings suggest sex-specific metabolic routing of PFAS effects, potentially involving microbiota-dependent mechanisms.

Mediation analysis further supported indirect effects of PFAS on metabolic pathways via steroids. Estradiol mediated associations with lithocholic acid, a hepatotoxic BA linked to

disease severity (Sen et al. 2024), whereas testosterone/epi-testosterone mediated associations with phospholipids previously associated with more favourable metabolic profiles (McGlinchey et al. 2022). These findings are consistent with our prior observations of stronger PFAS-associated metabolic disturbances in females (Sen et al. 2022).

Strengths of this study include comprehensive integration of clinical phenotyping with steroid profiling, lipidomics and BA analysis in a biopsy-characterised MASLD cohort. Limitations include the cross-sectional design and lack of detailed hormonal status information, particularly in women, which may influence steroid variability. In addition, PFAS and steroid measurements were obtained from serum, whereas lipid and BA profiles were derived from liver tissue.

In conclusion, our findings identify steroid hormones as potential key intermediates linking PFAS exposure to metabolic dysregulation in MASLD, with pronounced sex-specific patterns. These results provide a mechanistic framework for understanding environmental contributions to MASLD and highlight the importance of incorporating sex as a biological variable in both mechanistic studies and environmental health risk assessment.

References

Cherubini, A.; Della Torre, S.; Pelusi, S.; Valenti, L. Sexual dimorphism of metabolic dysfunction-associated steatotic liver disease. Trends Mol Med 2024;30:1126-1136

Cui, Q.; Pan, Y.; Wang, J.; Liu, H.; Yao, B.; Dai, J. Exposure to per- and polyfluoroalkyl substances (PFASs) in serum versus semen and their association with male reproductive hormones. Environmental Pollution 2020;266:115330

Deierlein, A.L.; Rock, S.; Park, S. Persistent Endocrine-Disrupting Chemicals and Fatty Liver Disease. Curr Environ Health Rep 2017;4:439-449

Dobre, M.Z.; Virgolici, B.; Cioarcă-Nedelcu, R. Lipid Hormones at the Intersection of Metabolic Imbalances and Endocrine Disorders. Curr Issues Mol Biol 2025;47

Eggert, A.; Cisneros-Montalvo, S.; Anandan, S.; Musilli, S.; Stukenborg, J.B.; Adamsson, A.; Nurmio, M.; Toppari, J. The effects of perfluorooctanoic acid (PFOA) on fetal and adult rat testis. Reprod Toxicol 2019;90:68-76

Foulds, C.E.; Treviño, L.S.; York, B.; Walker, C.L. Endocrine-disrupting chemicals and fatty liver disease. Nat Rev Endocrinol 2017;13:445-457

Frank, A.P.; de Souza Santos, R.; Palmer, B.F.; Clegg, D.J. Determinants of body fat distribution in humans may provide insight about obesity-related health risks. J Lipid Res 2019;60:1710-1719

Giulivo, M.; Lopez de Alda, M.; Capri, E.; Barceló, D. Human exposure to endocrine disrupting compounds: Their role in reproductive systems, metabolic syndrome and breast cancer. A review. Environ Res 2016;151:251-264

Heindel, J.J.; Blumberg, B.; Cave, M.; Machtinger, R.; Mantovani, A.; Mendez, M.A.; Nadal, A.; Palanza, P.; Panzica, G.; Sargis, R.; Vandenberg, L.N.; Vom Saal, F. Metabolism disrupting chemicals and metabolic disorders. Reprod Toxicol 2017;68:3-33

Henriksen, L.S.; Hagen, C.P.; Assens, M.; Busch, A.S.; Skakkebæk, N.E.; Almstrup, K.; Main, K.M. Genetic Variations in FSH Action Affect Sex Hormone Levels and Breast Tissue Size in Infant Girls: A Pilot Study. J Clin Endocrinol Metab 2016;101:3191-3198

India-Aldana, S.; Yao, M.; Midya, V.; Colicino, E.; Chatzi, L.; Chu, J.; Gennings, C.; Jones, D.P.; Loos, R.J.F.; Setiawan, V.W.; Smith, M.R.; Walker, R.W.; Barupal, D.; Walker, D.I.; Valvi,

D. PFAS Exposures and the Human Metabolome: A Systematic Review of Epidemiological Studies. Curr Pollut Rep 2023;9:510-568
Joensen, U.N.; Veyrand, B.; Antignac, J.-P.; Blomberg Jensen, M.; Petersen, J.H.; Marchand, P.; Skakkebæk, N.E.; Andersson, A.-M.; Le Bizec, B.; Jørgensen, N. PFOS (perfluorooctanesulfonate) in serum is negatively associated with testosterone levels, but not with semen quality, in healthy men. Human Reproduction 2013;28:599-608
Kang, J.S.; Choi, J.S.; Park, J.W. Transcriptional changes in steroidogenesis by perfluoroalkyl acids (PFOA and PFOS) regulate the synthesis of sex hormones in H295R cells. Chemosphere 2016;155:436-443
Kurz, S.A. Recoding Introduction to Mediation, Moderation, and Conditional Process Analysis. Bookdown; 2023
Kushnir, M.M.; Salihovic, S.; Bergquist, J.; Lind, P.M.; Lind, L. Environmental contaminants, sex hormones and SHBG in an elderly population. Environ Res 2024;263:120054
Lee, E.; Schumacher, F.; Lewinger, J.P.; Neuhausen, S.L.; Anton-Culver, H.; Horn-Ross, P.L.; Henderson, K.D.; Ziogas, A.; Van Den Berg, D.; Bernstein, L.; Ursin, G. The association of polymorphisms in hormone metabolism pathway genes, menopausal hormone therapy, and breast cancer risk: a nested case-control study in the California Teachers Study cohort. Breast Cancer Res 2011;13:R37
Lin, H.Y.; Yu, I.C.; Wang, R.S.; Chen, Y.T.; Liu, N.C.; Altuwaijri, S.; Hsu, C.L.; Ma, W.L.; Jokinen, J.; Sparks, J.D.; Yeh, S.; Chang, C. Increased hepatic steatosis and insulin resistance in mice lacking hepatic androgen receptor. Hepatology 2008;47:1924-1935
Luukkonen, P.K.; Zhou, Y.; Sadevirta, S.; Leivonen, M.; Arola, J.; Oresic, M.; Hyotylainen, T.; Yki-Jarvinen, H. Hepatic ceramides dissociate steatosis and insulin resistance in patients with non-alcoholic fatty liver disease. J Hepatol 2016;64:1167-1175
MacMillan, D.K.; Wetmore, B.A.; Dasgupta, S.; Baldwin, W.S. Closing the Gaps in Understanding PFAS Toxicology and Metabolism. Toxics 2024;13
Mårin, P. Testosterone and regional fat distribution. Obes Res 1995;3 Suppl 4:609s-612s
Mayneris-Perxachs, J.; Arnoriaga-Rodríguez, M.; Luque-Córdoba, D.; Priego-Capote, F.; Pérez-Brocal, V.; Moya, A.; Burokas, A.; Maldonado, R.; Fernández-Real, J.-M. Gut microbiota steroid sexual dimorphism and its impact on gonadal steroids: influences of obesity and menopausal status. Microbiome 2020;8:136
McGlinchey, A.J.; Govaere, O.; Geng, D.; Ratziu, V.; Allison, M.; Bousier, J.; Petta, S.; de Oliviera, C.; Bugianesi, E.; Schattenberg, J.M.; Daly, A.K.; Hyötyläinen, T.; Anstee, Q.M.; Orešič, M. Metabolic signatures across the full spectrum of non-alcoholic fatty liver disease. JHEP Rep 2022;4:100477
Münzker, J.; Hofer, D.; Trummer, C.; Ulbing, M.; Harger, A.; Pieber, T.; Owen, L.; Keevil, B.; Brabant, G.; Lerchbaum, E.; Obermayer-Pietsch, B. Testosterone to dihydrotestosterone ratio as a new biomarker for an adverse metabolic phenotype in the polycystic ovary syndrome. J Clin Endocrinol Metab 2015;100:653-660
Münzker, J.; Lindheim, L.; Adaway, J.; Trummer, C.; Lerchbaum, E.; Pieber, T.R.; Keevil, B.; Obermayer-Pietsch, B. High salivary testosterone-to-androstenedione ratio and adverse metabolic phenotypes in women with polycystic ovary syndrome. Clin Endocrinol (Oxf) 2017;86:567-575
Ortiz-Huidobro, R.I.; Velasco, M.; Larque, C.; Escalona, R.; Hiriart, M. Molecular Insulin Actions Are Sexually Dimorphic in Lipid Metabolism. Front Endocrinol (Lausanne) 2021;12:690484
Polyzos, S.A.; Targher, G. Role of Glucocorticoids in Metabolic Dysfunction-Associated Steatotic Liver Disease. Curr Obes Rep 2024;13:242-255

Quagliarini, F.; Makris, K.; Friano, M.E.; Uhlenhaut, N.H. EJE Prize 2023: genes on steroids-genomic control of hepatic metabolism by the glucocorticoid receptor. Eur J Endocrinol 2023;188:R111-r130

Ramos-Molina, B.; Rossell, J.; Pérez-Montes de Oca, A.; Pardina, E.; Genua, I.; Rojo-López, M.I.; Julián, M.T.; Alonso, N.; Julve, J.; Mauricio, D. Therapeutic implications for sphingolipid metabolism in metabolic dysfunction-associated steatohepatitis. Front Endocrinol (Lausanne) 2024;15:1400961

Saad, R.J.; Keenan, B.S.; Danadian, K.; Lewy, V.D.; Arslanian, S.A. Dihydrotestosterone treatment in adolescents with delayed puberty: does it explain insulin resistance of puberty? J Clin Endocrinol Metab 2001;86:4881-4886

Seidemann, L.; Lippold, C.P.; Rohm, C.M.; Eckel, J.C.; Schicht, G.; Matz-Soja, M.; Berg, T.; Seehofer, D.; Damm, G. Sex hormones differently regulate lipid metabolism genes in primary human hepatocytes. BMC Endocr Disord 2024;24:135

Sen, P.; Fan, Y.; Schlezinger, J.J.; Ehrlich, S.D.; Webster, T.F.; Hyötyläinen, T.; Pedersen, O.; Orešič, M. Exposure to environmental toxicants is associated with gut microbiome dysbiosis, insulin resistance and obesity. Environ Int 2024;186:108569

Sen, P.; Qadri, S.; Luukkonen, P.K.; Ragnarsdottir, O.; McGlinchey, A.; Jäntti, S.; Juuti, A.; Arola, J.; Schlezinger, J.J.; Webster, T.F.; Orešič, M.; Yki-Järvinen, H.; Hyötyläinen, T. Exposure to environmental contaminants is associated with altered hepatic lipid metabolism in non-alcoholic fatty liver disease. J Hepatol 2022;76:283-293

Shen, M.; Shi, H. Sex Hormones and Their Receptors Regulate Liver Energy Homeostasis. Int J Endocrinol 2015;2015:294278

Song, M.J.; Choi, J.Y. Androgen dysfunction in non-alcoholic fatty liver disease: Role of sex hormone binding globulin. Front Endocrinol (Lausanne) 2022;13:1053709

Syed-Abdul, M.M. Lipid Metabolism in Metabolic-Associated Steatotic Liver Disease (MASLD). Metabolites 2023;14

Tian, M.; Huang, Q.; Wang, H.; Martin, F.L.; Liu, L.; Zhang, J.; Shen, H. Biphasic effects of perfluorooctanoic acid on steroidogenesis in mouse Leydig tumour cells. Reprod Toxicol 2019;83:54-62

Treviño, L.S.; Katz, T.A. Endocrine Disruptors and Developmental Origins of Nonalcoholic Fatty Liver Disease. Endocrinology 2018;159:20-31

Vujkovic, M.; Ramdas, S.; Lorenz, K.M.; Guo, X.; Darlay, R.; Cordell, H.J.; He, J.; Gindin, Y.; Chung, C.; Myers, R.P.; Schneider, C.V.; Park, J.; Lee, K.M.; Serper, M.; Carr, R.M.; Kaplan, D.E.; Haas, M.E.; MacLean, M.T.; Witschey, W.R.; Zhu, X.; Tcheandjieu, C.; Kember, R.L.; Kranzler, H.R.; Verma, A.; Giri, A.; Klarin, D.M.; Sun, Y.V.; Huang, J.; Huffman, J.E.; Creasy, K.T.; Hand, N.J.; Liu, C.T.; Long, M.T.; Yao, J.; Budoff, M.; Tan, J.; Li, X.; Lin, H.J.; Chen, Y.I.; Taylor, K.D.; Chang, R.K.; Krauss, R.M.; Vilarinho, S.; Brancale, J.; Nielsen, J.B.; Locke, A.E.; Jones, M.B.; Verweij, N.; Baras, A.; Reddy, K.R.; Neuschwander-Tetri, B.A.; Schwimmer, J.B.; Sanyal, A.J.; Chalasani, N.; Ryan, K.A.; Mitchell, B.D.; Gill, D.; Wells, A.D.; Manduchi, E.; Saiman, Y.; Mahmud, N.; Miller, D.R.; Reaven, P.D.; Phillips, L.S.; Muralidhar, S.; DuVall, S.L.; Lee, J.S.; Assimes, T.L.; Pyarajan, S.; Cho, K.; Edwards, T.L.; Damrauer, S.M.; Wilson, P.W.; Gaziano, J.M.; O'Donnell, C.J.; Khera, A.V.; Grant, S.F.A.; Brown, C.D.; Tsao, P.S.; Saleheen, D.; Lotta, L.A.; Bastarache, L.; Anstee, Q.M.; Daly, A.K.; Meigs, J.B.; Rotter, J.I.; Lynch, J.A.; Rader, D.J.; Voight, B.F.; Chang, K.M. A multiancestry genome-wide association study of unexplained chronic ALT elevation as a proxy for nonalcoholic fatty liver disease with histological and radiological validation. Nat Genet 2022;54:761-771

Wahlang, B.; Jin, J.; Beier, J.I.; Hardesty, J.E.; Daly, E.F.; Schnegelberger, R.D.; Falkner, K.C.; Prough, R.A.; Kirpich, I.A.; Cave, M.C. Mechanisms of Environmental Contributions to Fatty Liver Disease. Curr Environ Health Rep 2019;6:80-94

Walker, J.A. Applied Statistics for Experimental Biology. 2024

Wang, Y.; Aimuzi, R.; Nian, M.; Zhang, Y.; Luo, K.; Zhang, J. Perfluoroalkyl substances and sex hormones in postmenopausal women: NHANES 2013-2016. Environ Int 2021;149:106408

Yang, J.D.; Abdelmalek, M.F.; Guy, C.D.; Gill, R.M.; Lavine, J.E.; Yates, K.; Klair, J.; Terrault, N.A.; Clark, J.M.; Unalp-Arida, A.; Diehl, A.M.; Suzuki, A. Patient Sex, Reproductive Status, and Synthetic Hormone Use Associate With Histologic Severity of Nonalcoholic Steatohepatitis. Clin Gastroenterol Hepatol 2017;15:127-131.e122

Yang, J.D.; Abdelmalek, M.F.; Pang, H.; Guy, C.D.; Smith, A.D.; Diehl, A.M.; Suzuki, A. Gender and menopause impact severity of fibrosis among patients with nonalcoholic steatohepatitis. Hepatology 2014;59:1406-1414

Yang, M.; Ma, F.; Guan, M. Role of Steroid Hormones in the Pathogenesis of Nonalcoholic Fatty Liver Disease. Metabolites 2021;11

Younossi, Z.M.; Golabi, P.; Paik, J.M.; Henry, A.; Van Dongen, C.; Henry, L. The global epidemiology of nonalcoholic fatty liver disease (NAFLD) and nonalcoholic steatohepatitis (NASH): a systematic review. Hepatology 2023;77:1335-1347

Zhang, J.; Cheng, X.; Wang, Y.; Guo, H.; Liu, L.; Liu, L.; Gao, J.; He, M. Association between serum per- and polyfluoroalkyl substances levels and metabolic dysfunction-associated steatotic liver disease. Environ Pollut 2024;363:125233

Zhou, Y.; Hu, L.W.; Qian, Z.M.; Geiger, S.D.; Parrish, K.L.; Dharmage, S.C.; Campbell, B.; Roponen, M.; Jalava, P.; Hirvonen, M.R.; Heinrich, J.; Zeng, X.W.; Yang, B.Y.; Qin, X.D.; Lee, Y.L.; Dong, G.H. Interaction effects of polyfluoroalkyl substances and sex steroid hormones on asthma among children. Sci Rep 2017;7:899

Tables

Table 1. The subject sizes in each case (steatosis, fibrosis, necroinflammation HOMA-IR) of this study. In addition to the overall case (HOMA-IR case level > 1.5 (Sen et al. 2022), and other cases (steatosis, fibrosis, necroinflammation) > 0) and control (≤ 1.5 or 0, respectively) group sizes, the study groups have been also subdivided to females and males.

	Steatosis			Fibrosis		
	All	**Females**	**Males**	**All**	**Females**	**Males**
Control	83	58	25	62	43	19
Case	21	11	10	42	26	16
	Necroinflammation			**HOMA-IR**		
Control	88	60	28	18	13	5
Case	16	9	7	86	56	30

Figure legends

Fig. 1. Steroid hormone concentrations in relation to steatosis. Log2-transformed plasma steroid levels in females (**A**) and males (**B**) stratified by steatosis status. Significant differences between groups are indicated (*p<0.1, **p<0.05, ***p<0.01, ****p<0.001; Wilcoxon test). The abbreviations of steroids: 11-Ketotestosterone (11-KT), 11b-OH-Androstenedione (11b-OH4), 11-Ketodihydrotestosterone (11-KDHT), 11-Ketoandrostenedione (11-KA4), Dehydroepiandrosterone (DHEA), Testosterone / (&) Epi-testosterone (T/Epi-T), Androsterone (AN), Dihydrotestosterone (DHT), Androstenedione (A4), Estradiol (E2), Estrone (E1), Cortisone (E), 11-Deoxycortisol (S), Corticosterone (B), Aldosterone (A), 17a-OH-Pregnenolone (17a-OHP5), 17a-OH-Progesterone (17a-OHP4), 11-Deoxycorticosterone (DOC), Pregnenolone (P5), Progesterone (P4), Estrogens (Est.), Glucocorticosteroids (Gl.), mineralcorticosteroids (Min.) and Progesterones (Proges.).

Fig. 2. Associations between PFAS exposure, steroid hormones and clinical covariates. Linear model estimates are shown for females and males separately. Models were adjusted for age, BMI and sex where appropriate. Statistical significance is indicated (*p<0.05, **p<0.01, ***p<0.001).

Fig. 3. **Associations between steroid hormones, bile acids and lipid classes.** Heatmap of scaled linear model estimates (range −0.5 to 0.5) for associations between clinical variables, steroids, bile acids and lipid classes in females and males. Models adjusted for age, BMI and sex where appropriate.

Fig. 4. Network representation of associations between PFAS, steroids, bile acids, lipids and clinical variables. Chord diagram showing significant partial correlations (Spearman; NRR<0.03). Only strongest associations are displayed.

Fig. 5. Causal mediation analysis of PFAS effects on metabolic pathways via steroid hormones. (**A**) Conceptual framework of mediation analysis, with two illustrative examples. (**B**) Sankey diagram illustrating indirect (ACME) and direct (ADE) effects of PFAS on lipid and bile acid outcomes mediated by steroid hormones. Only associations with p<0.1 are shown.

Fig. 1

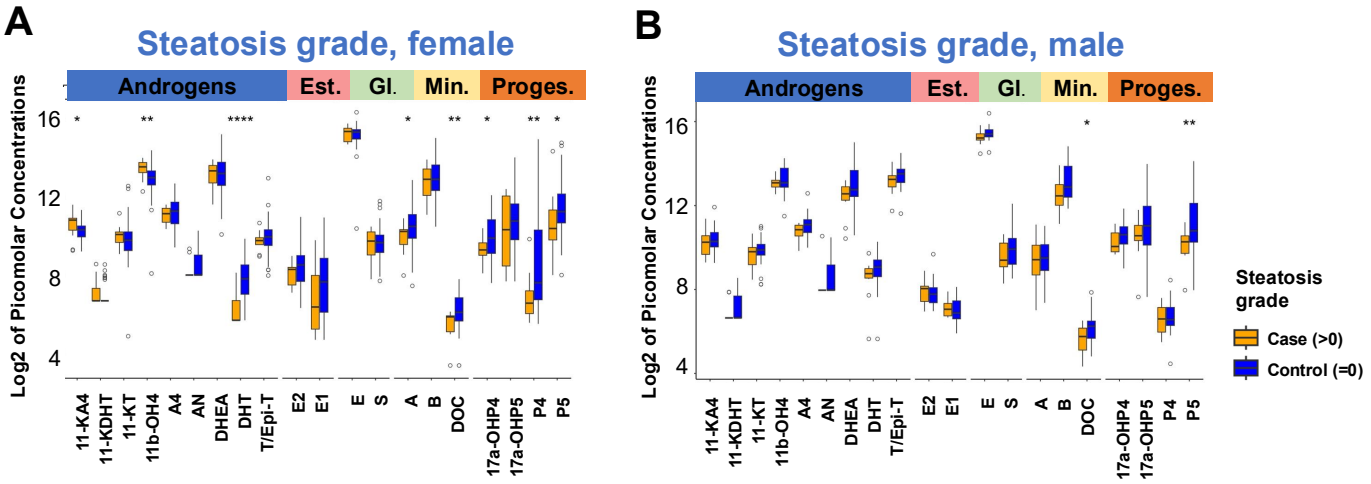
A
Steatosis grade, female
Androgens
Est.
Gl.
Min.
Proges.
Log2 of Picomolar Concentrations
16
12
8
4
11-KA4
11-KDHT
11-KT
11b-OH4
A4
AN
DHEA
DHT
T/Epi-T
E2
E1
E
S
A
B
DOC
17a-OHP4
17a-OHP5
P4
P5
B
Steatosis grade, male
Steatosis grade
Case (>0)
Control (=0)

Fig. 2

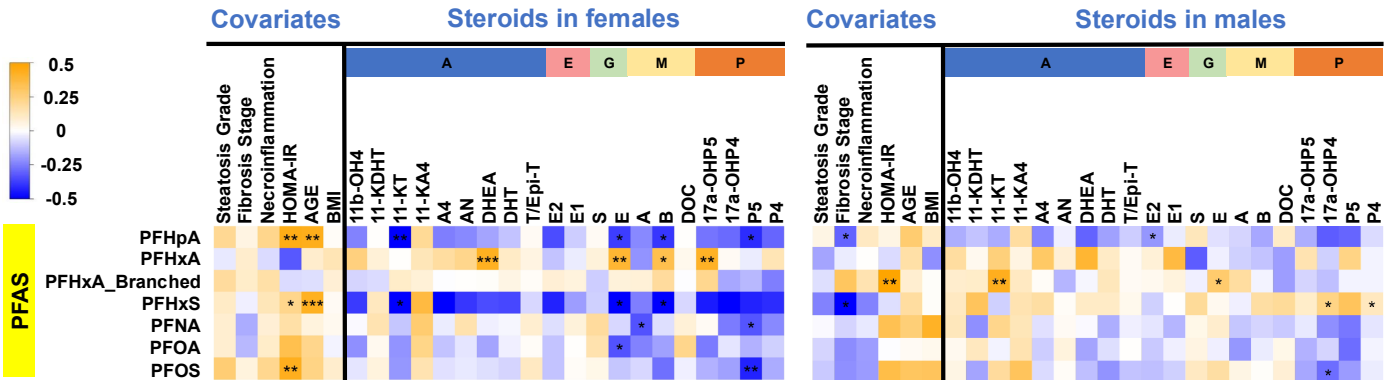
Covariates
Steroids in females
Covariates
Steroids in males
0.5
0.25
0
-0.25
-0.5
PFAS
PFHpA
PFHxA
PFHxA_Branched
PFHxS
PFNA
PFOA
PFOS
Steatosis Grade
Fibrosis Stage
Necroinflammation
HOMA-IR
AGE
BMI
11b-OH4
11-KDHT
11-KT
11-KA4
A4
AN
DHEA
DHT
T/Epi-T
E2
E1
S
E
A
B
DOC
17a-OHP5
17a-OHP4
P5
P4
A
E
G
M
P

Fig 3.

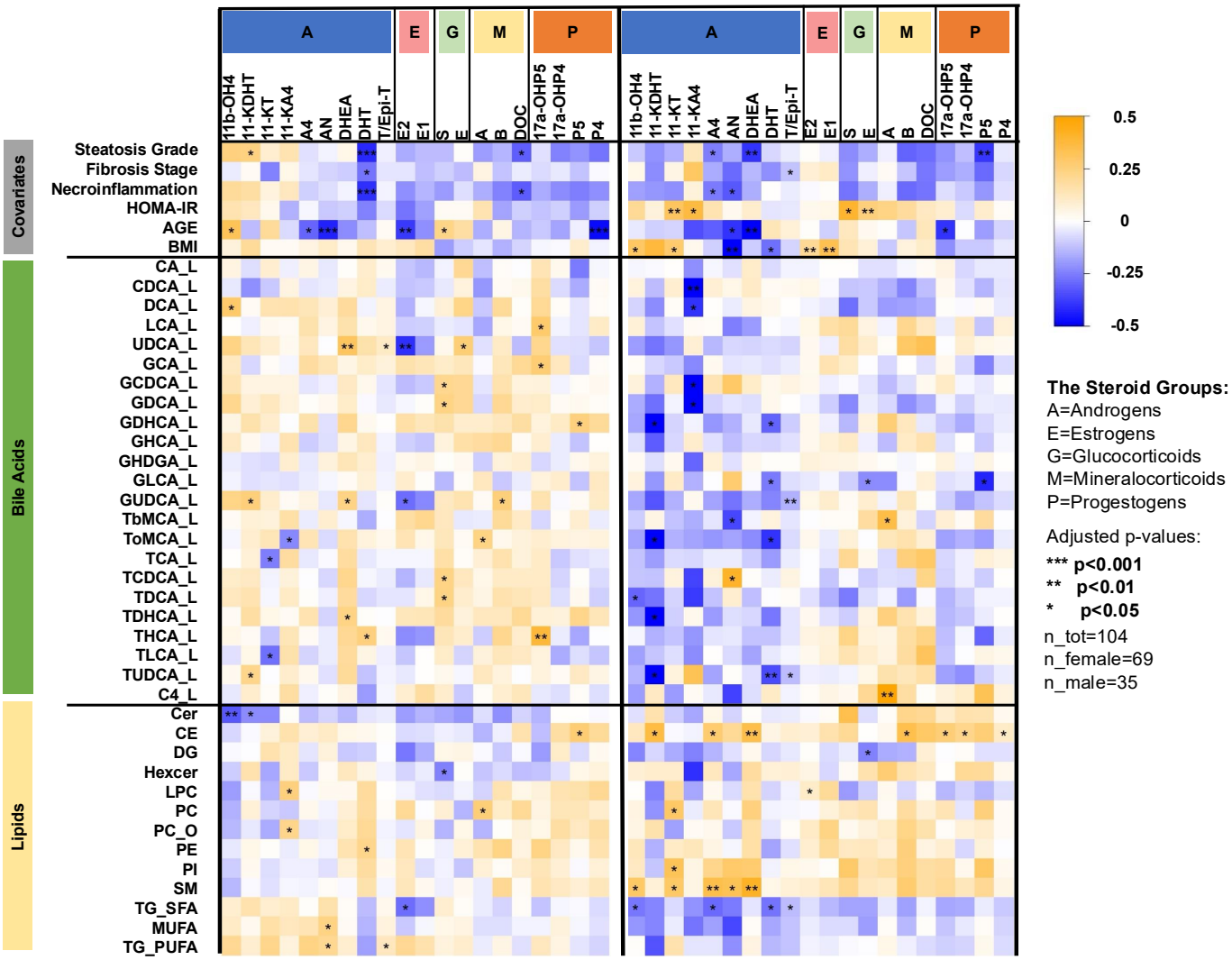
A
E
G
M
P
11b-OH4
11-KDHT
11-KT
11-KA4
A4
AN
DHEA
DHT
T/Epi-T
E2
E1
S
E
A
B
DOC
17a-OHP5
17a-OHP4
P5
P4
Covariates
Steatosis Grade
Fibrosis Stage
Necroinflammation
HOMA-IR
AGE
BMI
Bile Acids
CA_L
CDCA_L
DCA_L
LCA_L
UDCA_L
GCA_L
GCDCA_L
GDCA_L
GDHCA_L
GHCA_L
GHDGA_L
GLCA_L
GUDCA_L
TbMCA_L
ToMCA_L
TCA_L
TCDCA_L
TDCA_L
TDHCA_L
THCA_L
TLCA_L
TUDCA_L
C4_L
Lipids
Cer
CE
DG
Hexcer
LPC
PC
PC_O
PE
PI
SM
TG_SFA
MUFA
TG_PUFA
0.5
0.25
0
-0.25
-0.5
The Steroid Groups:
A=Androgens
E=Estrogens
G=Glucocorticoids
M=Mineralocorticoids
P=Progestogens
Adjusted p-values:
*** p<0.001
** p<0.01
* p<0.05
n_tot=104
n_female=69
n_male=35

Fig 4.

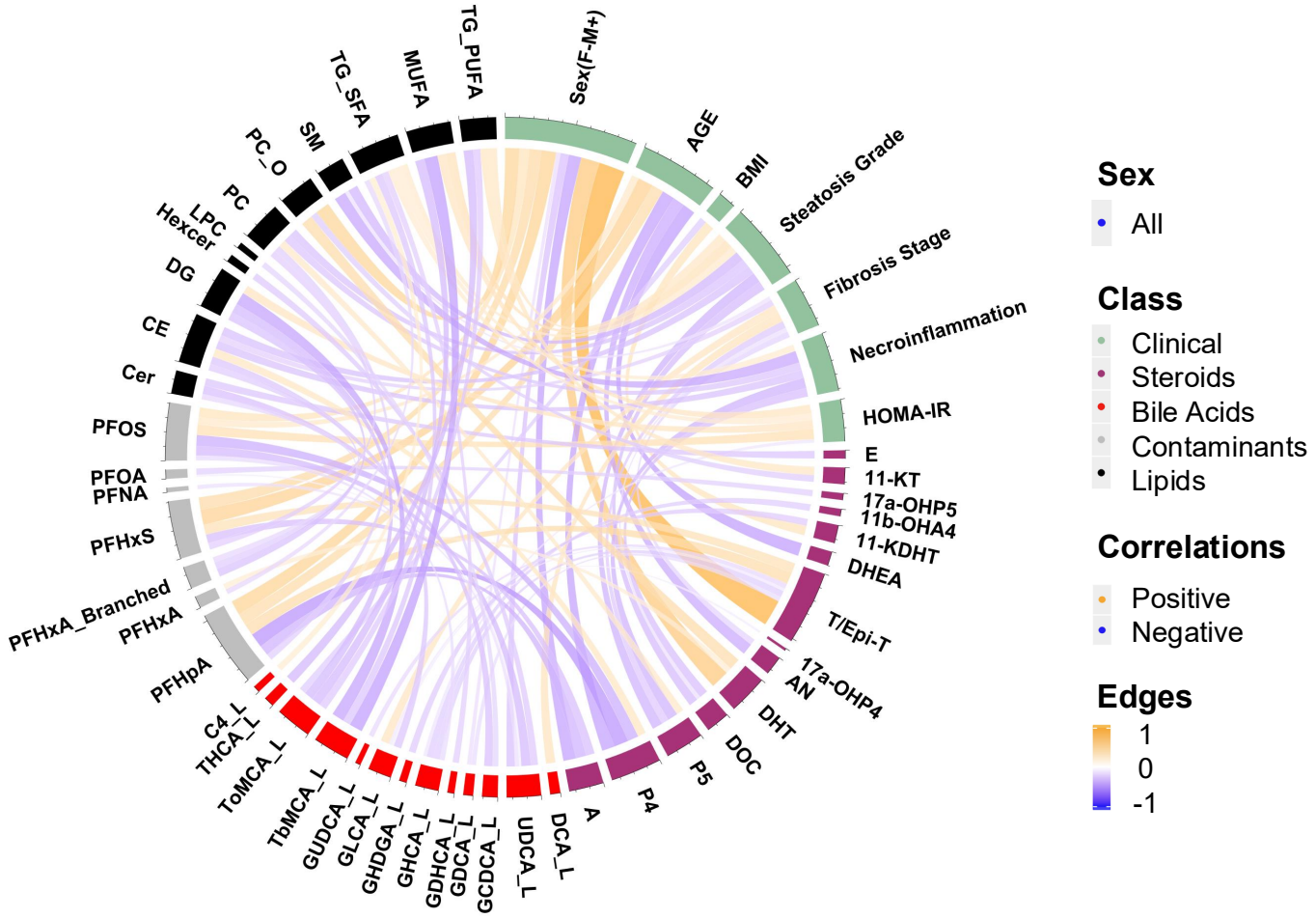
TG_PUFA
MUFA
TG_SFA
SM
PC_O
PC
LPC
Hexcer
DG
CE
Cer
PFOS
PFOA
PFNA
PFHxS
PFHxA_Branched
PFHxA
PFHpA
C4_L
THCA_L
ToMCA_L
TbMCA_L
GUDCA_L
GLCA_L
GHDGA_L
GHCA_L
GDHCA_L
GDCA_L
GCDCA_L
UDCA_L
DCA_L
A
P4
P5
DOC
DHT
AN
17a-OHP4
T/Epi-T
DHEA
11-KDHT
11b-OHA4
17a-OHP5
11-KT
E
HOMA-IR
Necroinflammation
Fibrosis Stage
Steatosis Grade
BMI
AGE
Sex(F-M+)
Sex
All
Class
Clinical
Steroids
Bile Acids
Contaminants
Lipids
Correlations
Positive
Negative
Edges
1
0
-1

Fig. 5

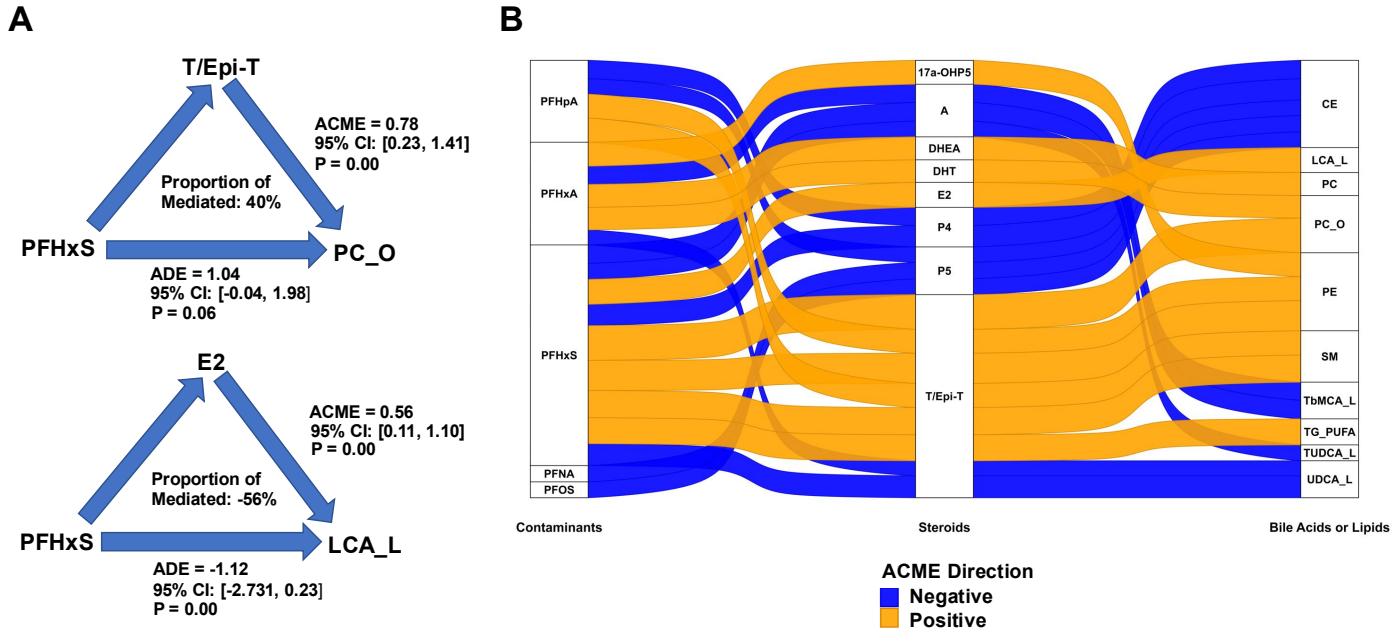
A
T/Epi-T
ACME = 0.78
95% CI: [0.23, 1.41]
P = 0.00
Proportion of
Mediated: 40%
PFHxS
PC_O
ADE = 1.04
95% CI: [-0.04, 1.98]
P = 0.06
E2
ACME = 0.56
95% CI: [0.11, 1.10]
P = 0.00
Proportion of
Mediated: -56%
PFHxS
LCA_L
ADE = -1.12
95% CI: [-2.731, 0.23]
P = 0.00
B
PFHpA
PFHxA
PFHxS
PFNA
PFOS
17a-OHP5
A
DHEA
DHT
E2
P4
P5
T/Epi-T
CE
LCA_L
PC
PC_O
PE
SM
TbMCA_L
TG_PUFA
TUDCA_L
UDCA_L
Contaminants
Steroids
Bile Acids or Lipids
ACME Direction
Negative
Positive

A PFAS-steroid axis is associated with lipid and bile acid metabolism in MASLD

Pauli Tikka, Aidan McGlinchey, Sami F. Qadri, Ilia Evstafev, Alex M. Dickens, Hannele Yki-Järvinen, Tuulia Hyötyläinen, Matej Orešič

Table of Contents

Supplementary figures **2**
Supplementary tables **17**

Supplementary figures

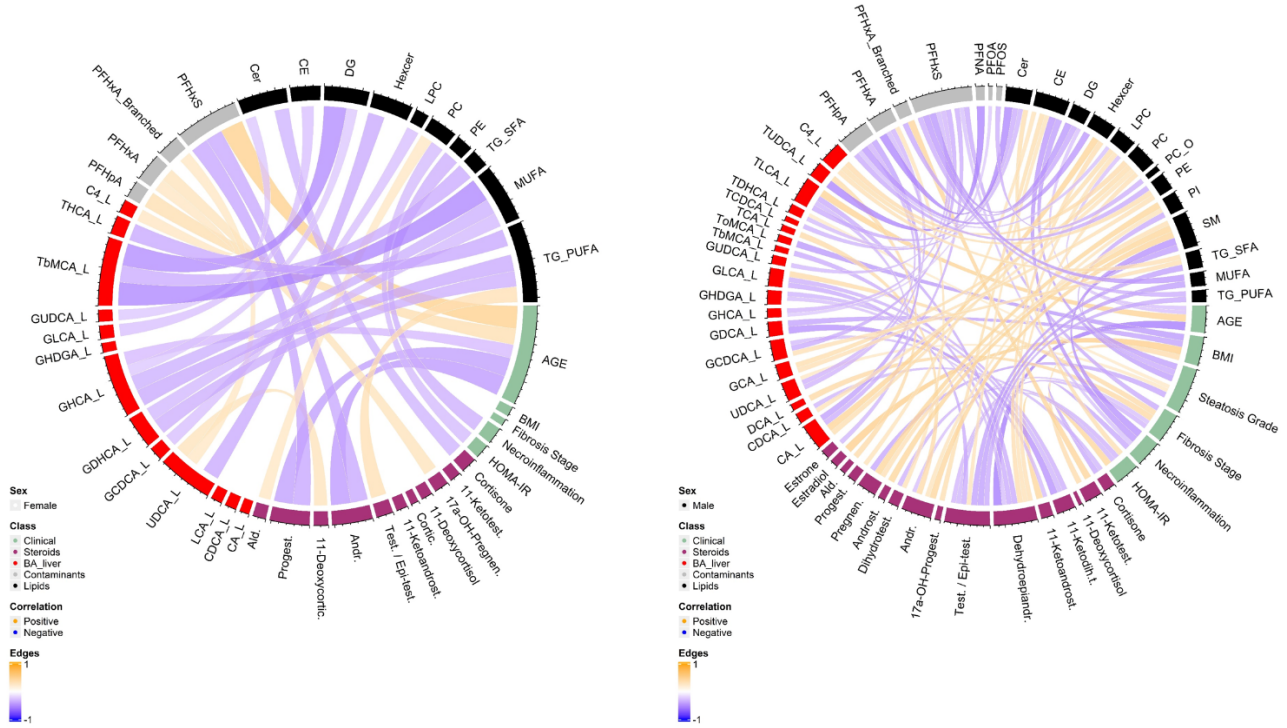

Fig. S1. Chord plot with significantly correlated (NRR<0.01) data of female and male subjects.

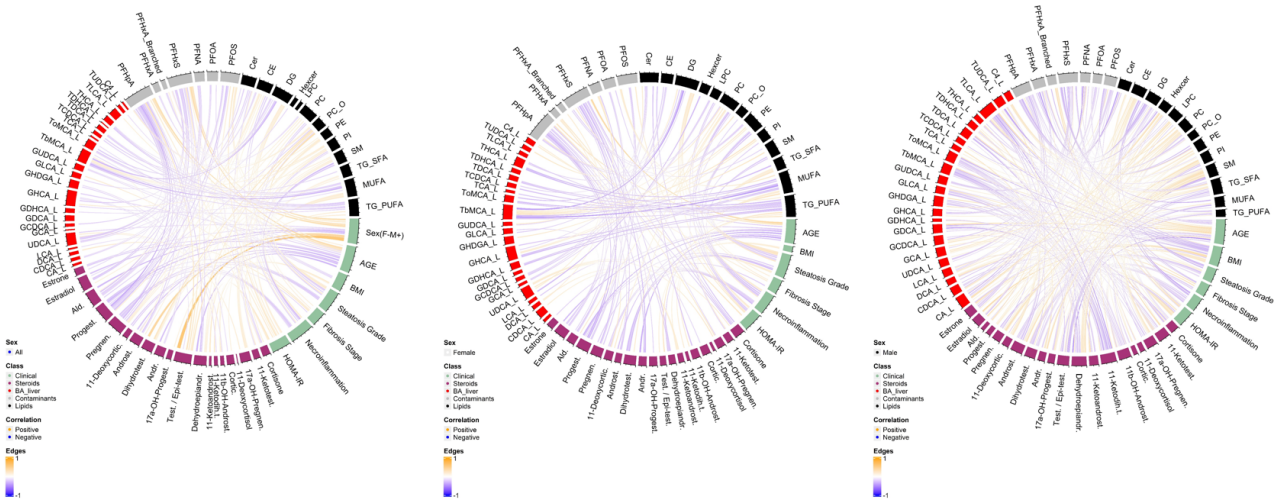

Fig. S2. A chord plot with significantly correlated (NRR<0.2) data of all, female and male subjects.

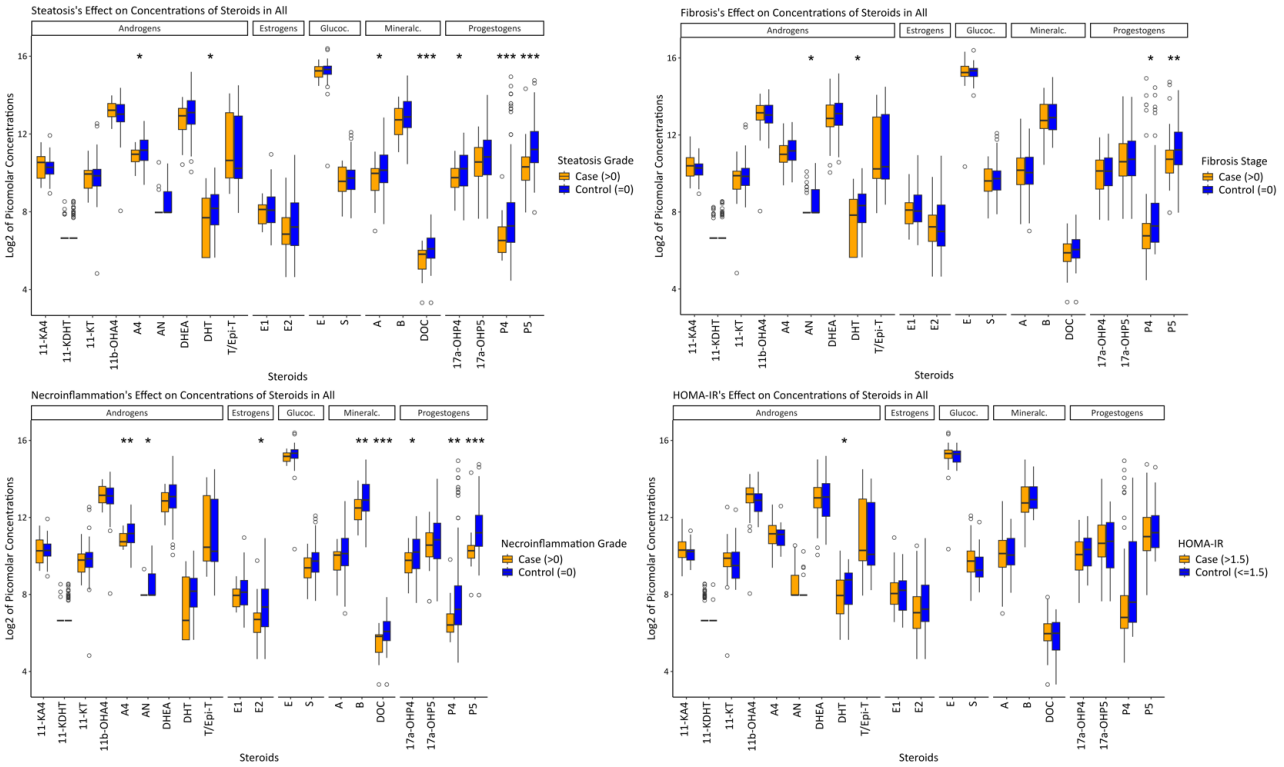

Fig. S3. Log2 of the picomolar concentrations of steroids in the all subjects of the cases (Steatosis, Necroinflammation, Fibrosis, HOMA-IR). The cases (orange) and controls (blue) are defined at **Fig. 1**. The significant steroids as per the linear models are marked with an asterisk (*).

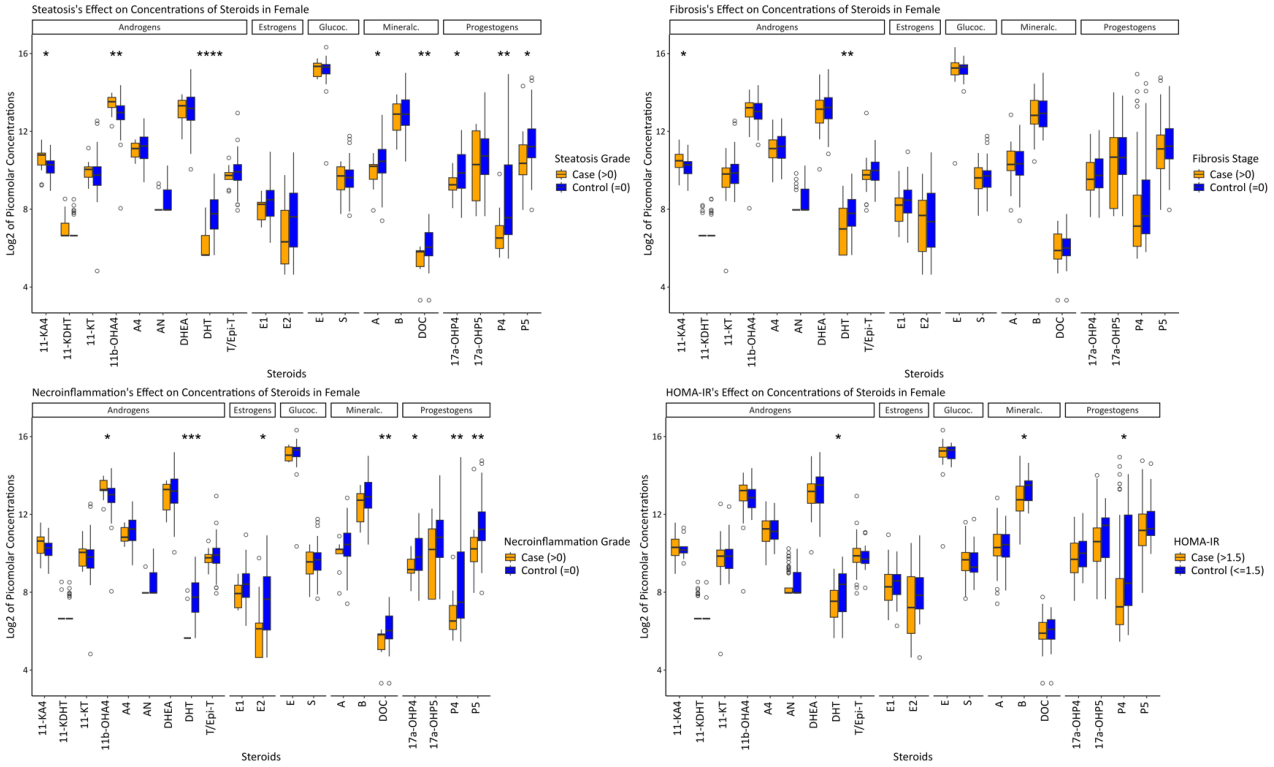

Fig. S4. Log2 of the picomolar concentrations of steroids in the female subjects of the cases (Steatosis, Necroinflammation, Fibrosis, HOMA-IR). The cases (orange) and controls (blue) are defined at **Fig. 1**. The significant steroids as per the linear models are marked with an asterisk (*).

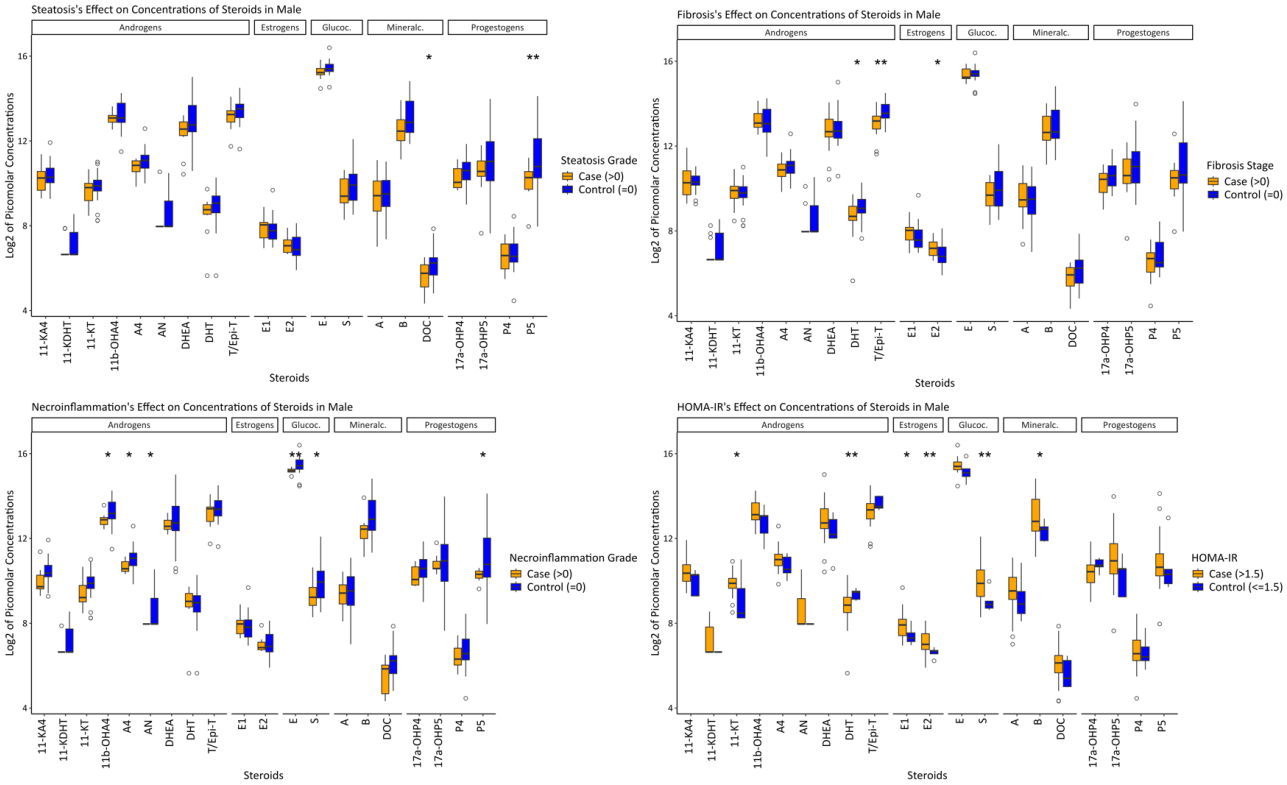

Fig. S5. Log2 of the picomolar concentrations of steroids in the male subjects of the cases (Steatosis, Necroinflammation, Fibrosis, HOMA-IR). The cases (orange) and controls (blue) are defined at **Fig. 1**. The significant steroids as per the linear models are marked with an asterisk (*).

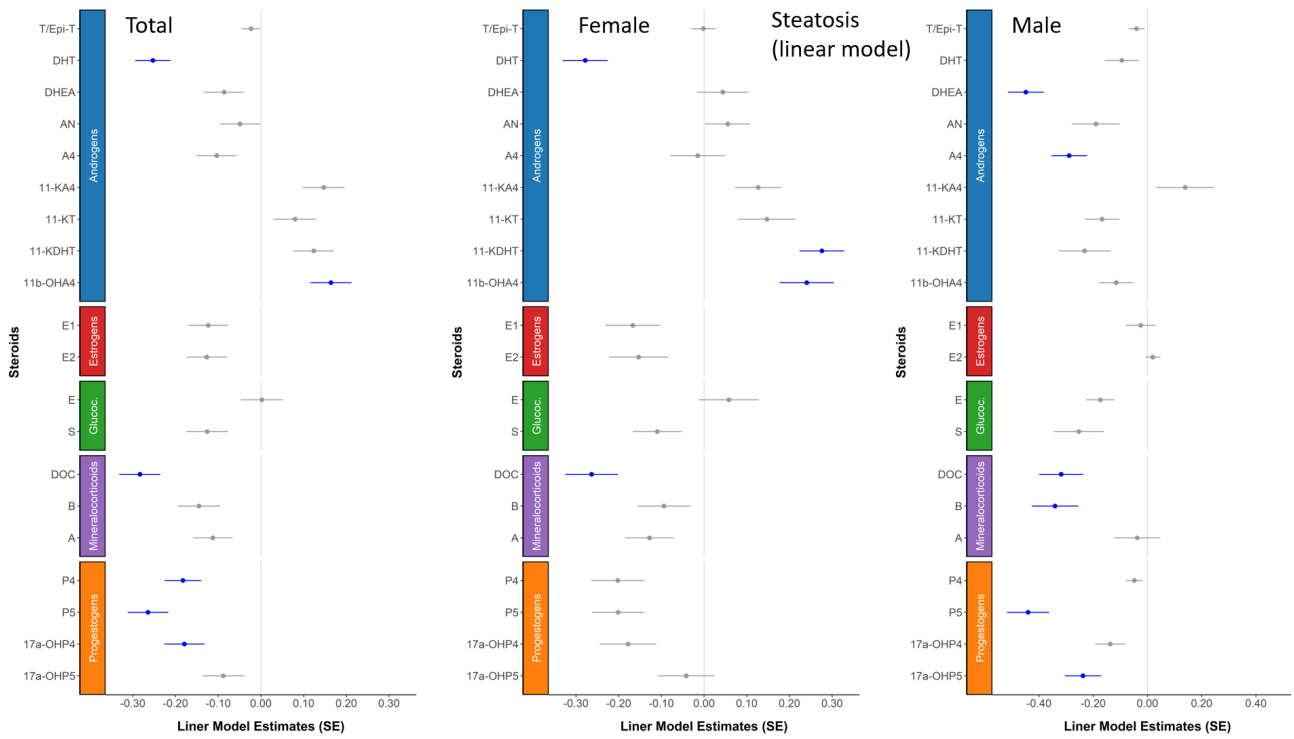

Fig. S6. The association of steatosis on steroids. The data was shown in three groups: all subjects, female and male subjects. Linear model coefficients and the adjusted significances (Age, BMI, gender) were derived with MaasLin2 R package (**Table S11**).

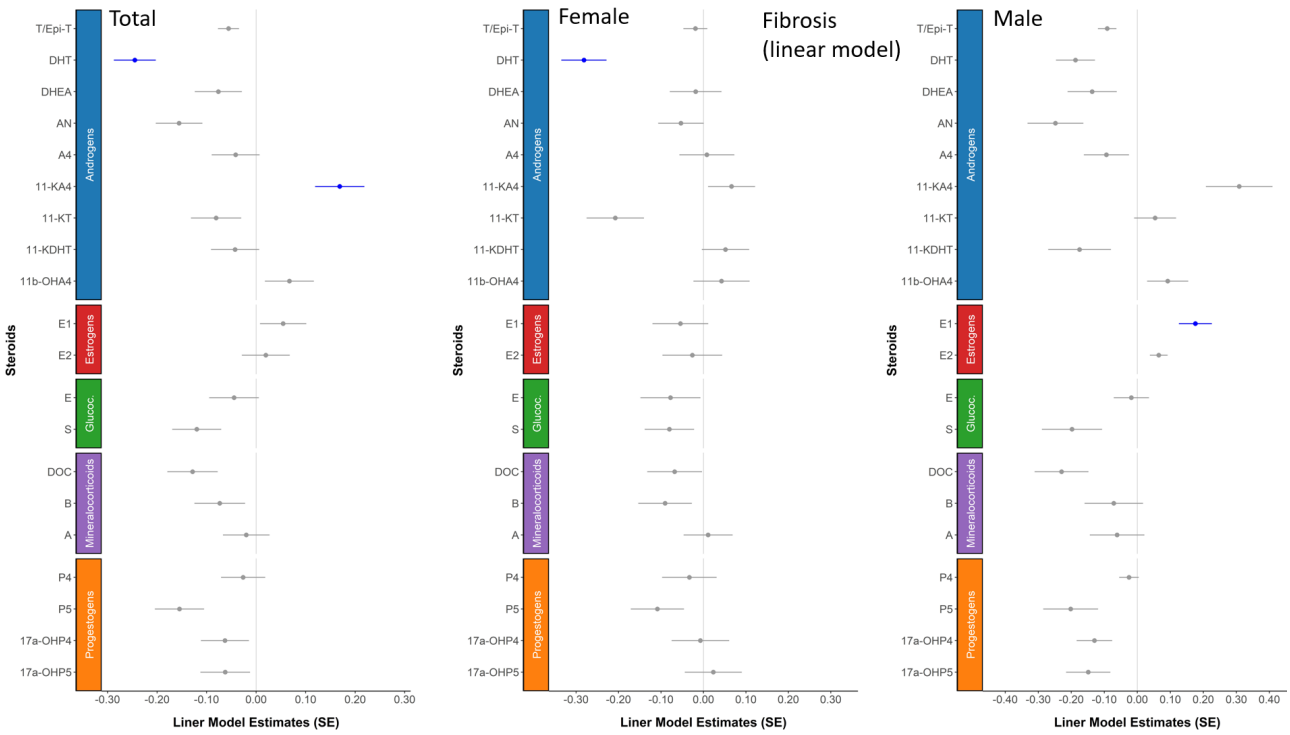

Fig. S7. The association of fibrosis on steroids. The data was shown in three groups: all subjects, female and male subjects. Linear model coefficients and the adjusted significances (Age, BMI, gender) were derived with MaasLin2 R package (**Table S11**).

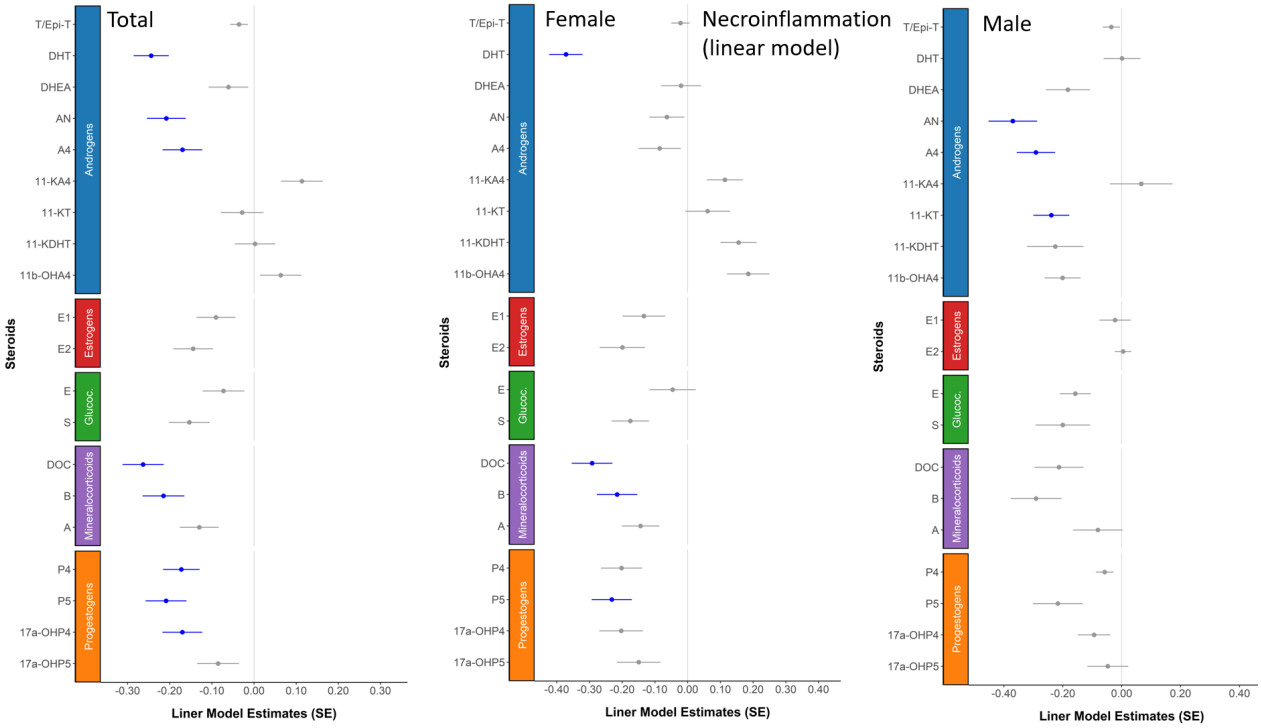

Fig. S8. The association of necroinflammation on steroids. The data was shown in three groups: all subjects, female and male subjects. Linear model coefficients and the adjusted significances (Age, BMI, gender) were derived with MaasLin2 R package (**Table S11**).

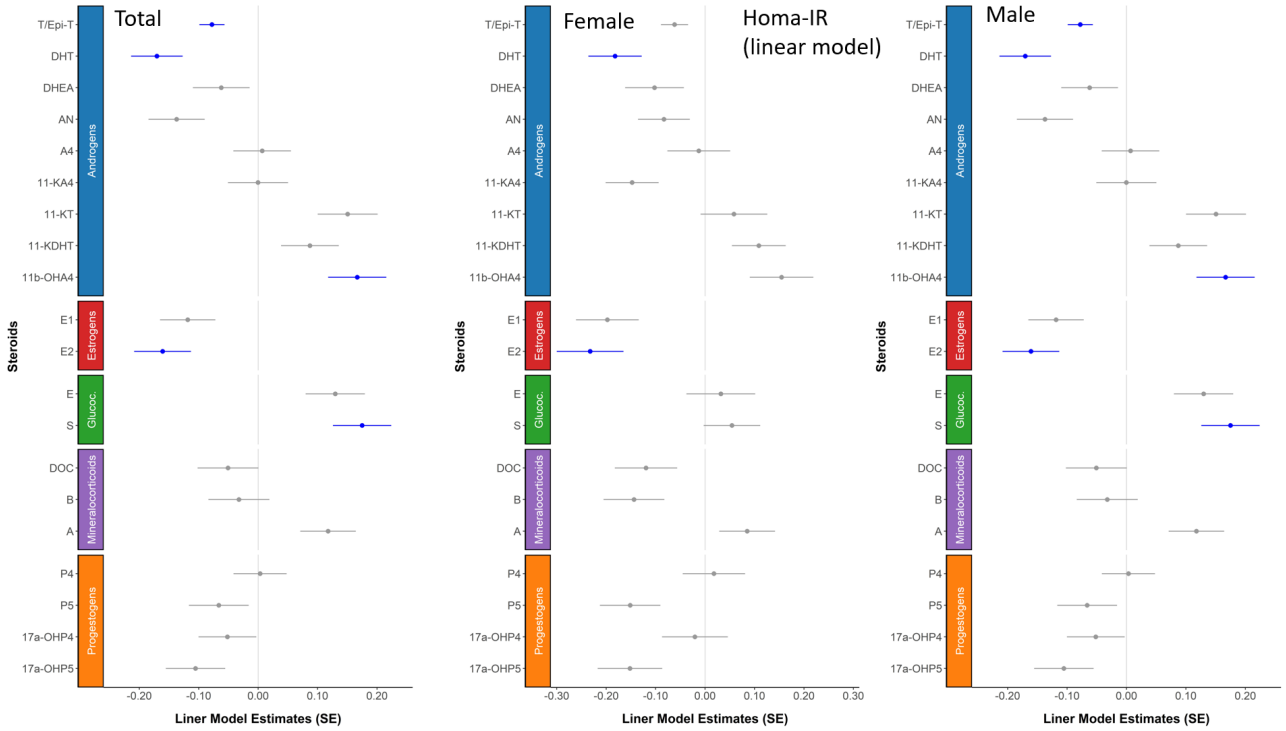

Fig. S9. The association of HOMA-IR on steroids. The data was shown in three groups: all subjects, female and male subjects. Linear model coefficients and the adjusted significances (Age, BMI, gender) were derived with MaasLin2 R package (**Table S11**).

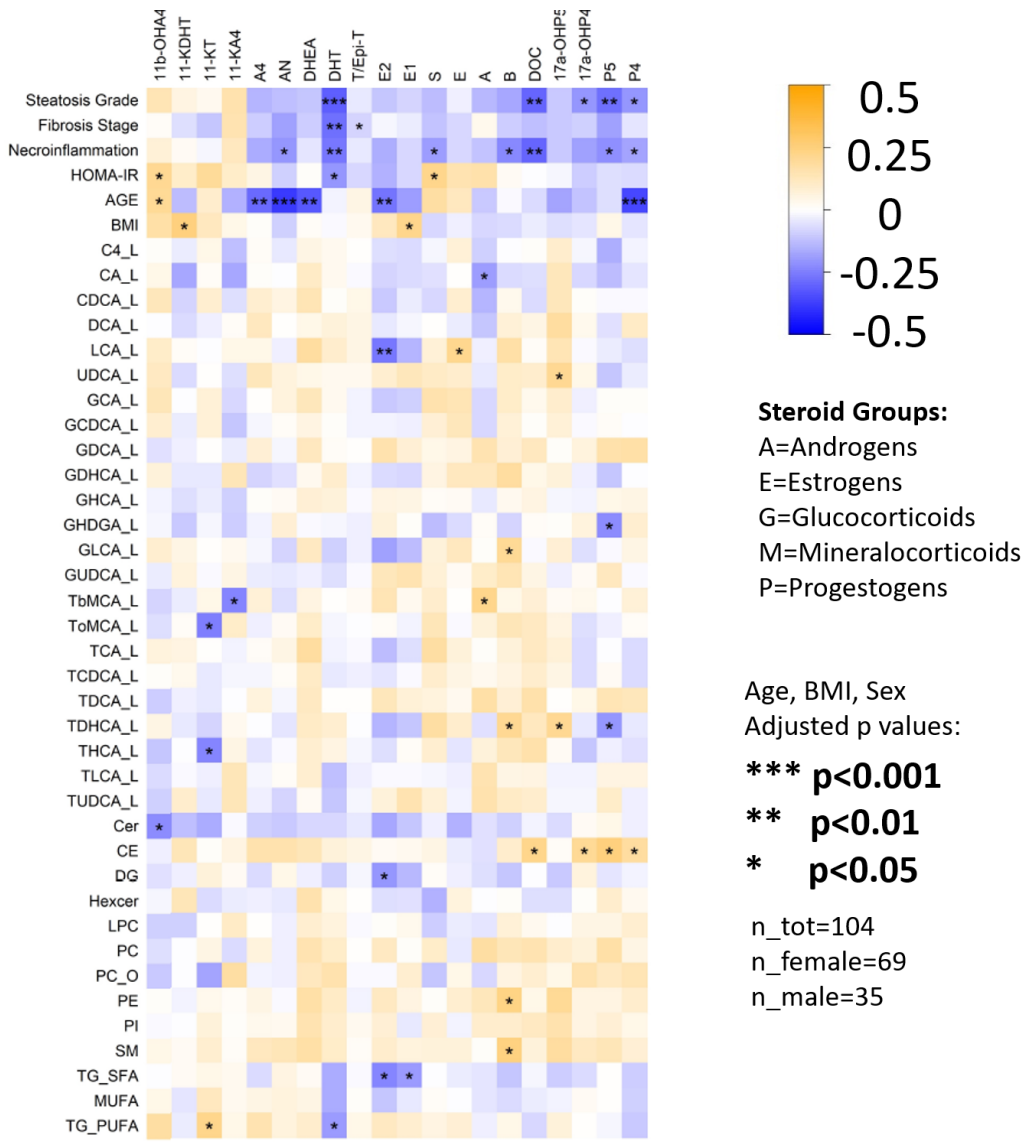

Figure S10. Linear model estimates between clinical covariates, bile acids, lipids and steroids in all subjects. The estimates were scaled between a range (-0.5 to 0.5) and the blue is a negative and red is a positive association. The confounders (age, BMI and sex*)* were added to the models when applicable. The p-values were obtained from the summary function (in R) with the models (via t tests; ***p<0.001, **p<0.01, *p<0.05). Steroid abbreviations are as in **Fig. 1**.

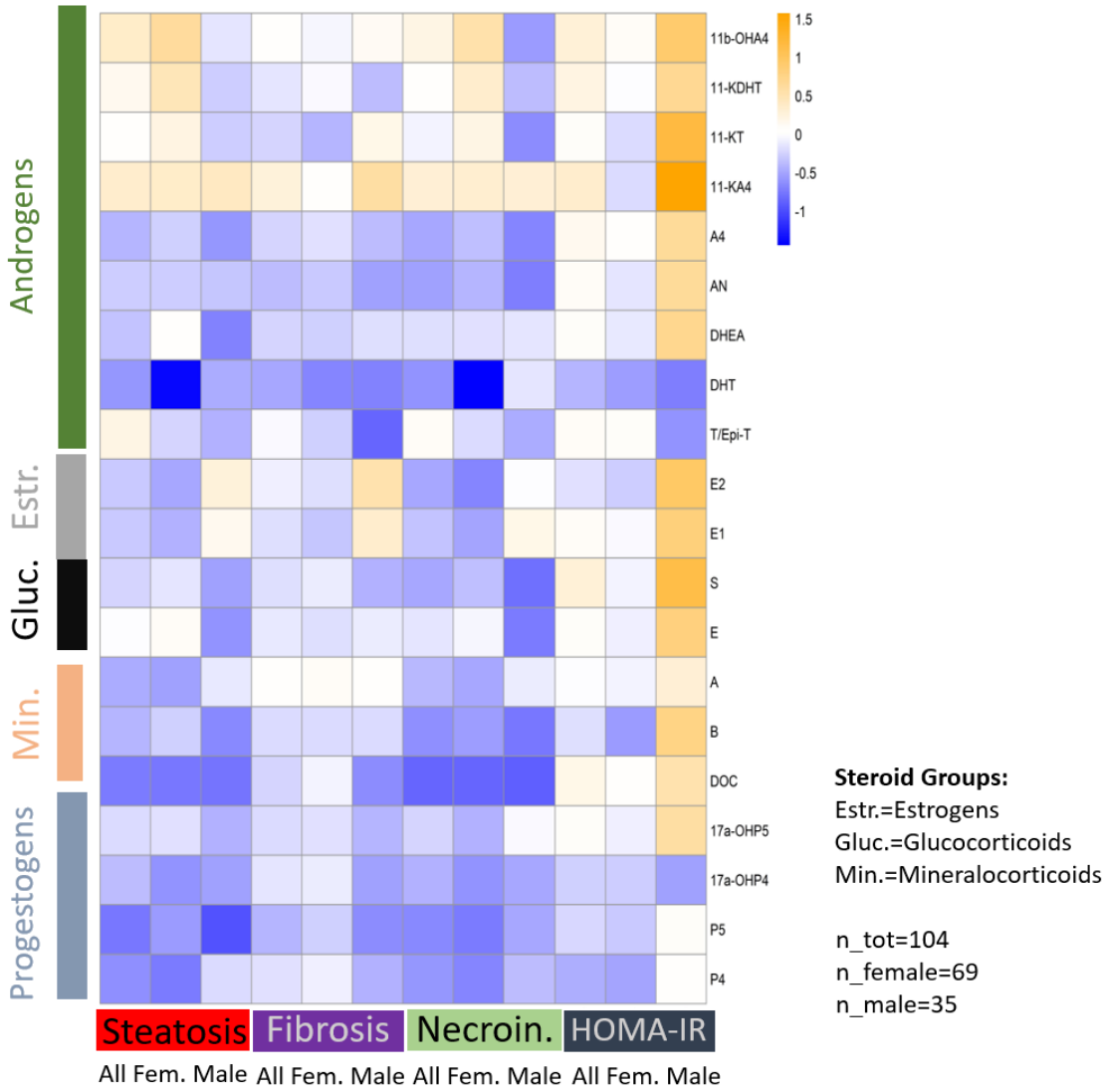

Fig. S11. Effect sizes in each group and sex.

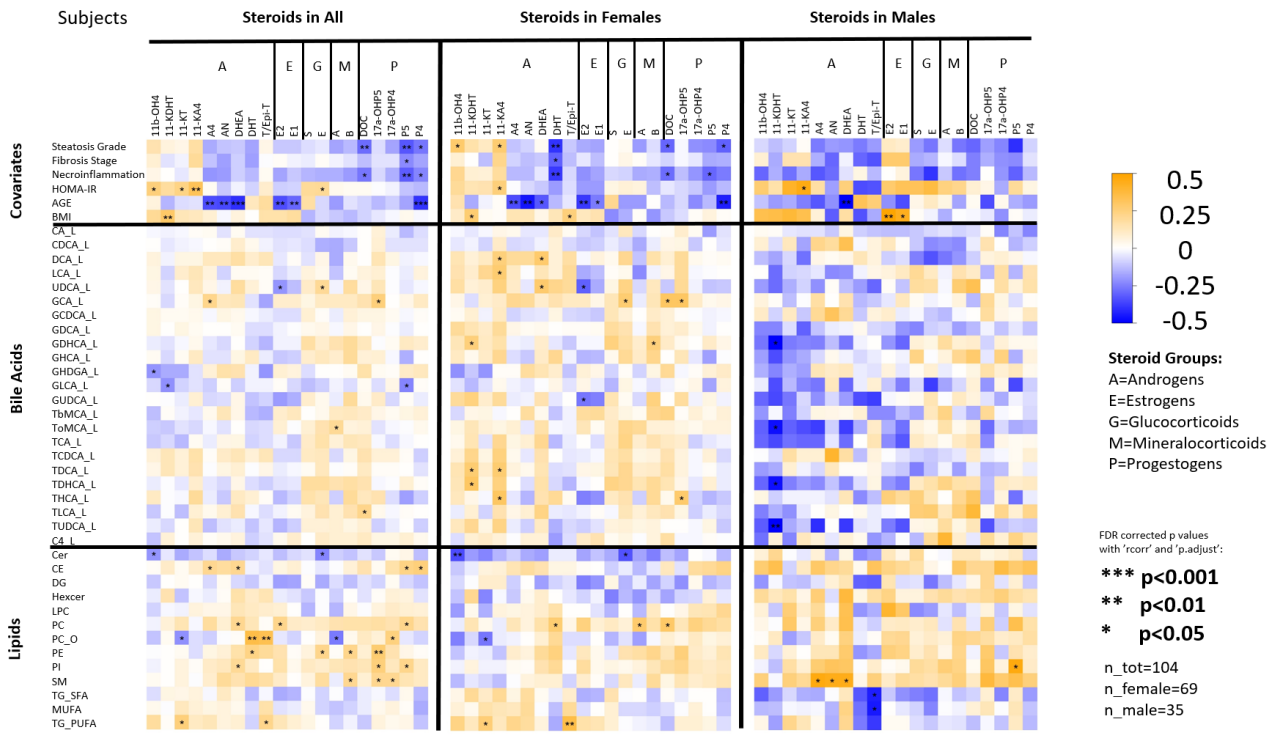

Fig. S12. Correlation coefficients (Spearman) between bile acids, lipids, clinical covariates and steroids. The coefficients were scaled between a range (-0.5 to 0.5) for a visual comparison and the blue is a negative and red is a positive association. Panels were done with the corrplot function (in R). The p values have been corrected for multiple testing. *****p<0.001, **p<0.05, *p<0.2.**

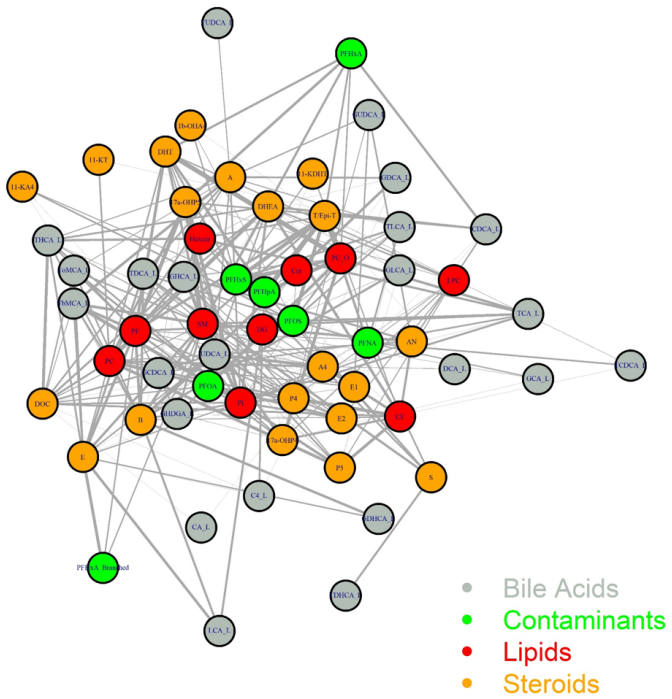

Fig. S13. Network plot done with iGraph and network functions (in R) using all samples' correlations with NRR=0.3 cut-off. The sizes of edges correspond the relative correlation strengths between the vertices. The vertex size is 0.3 times the degree of the network.

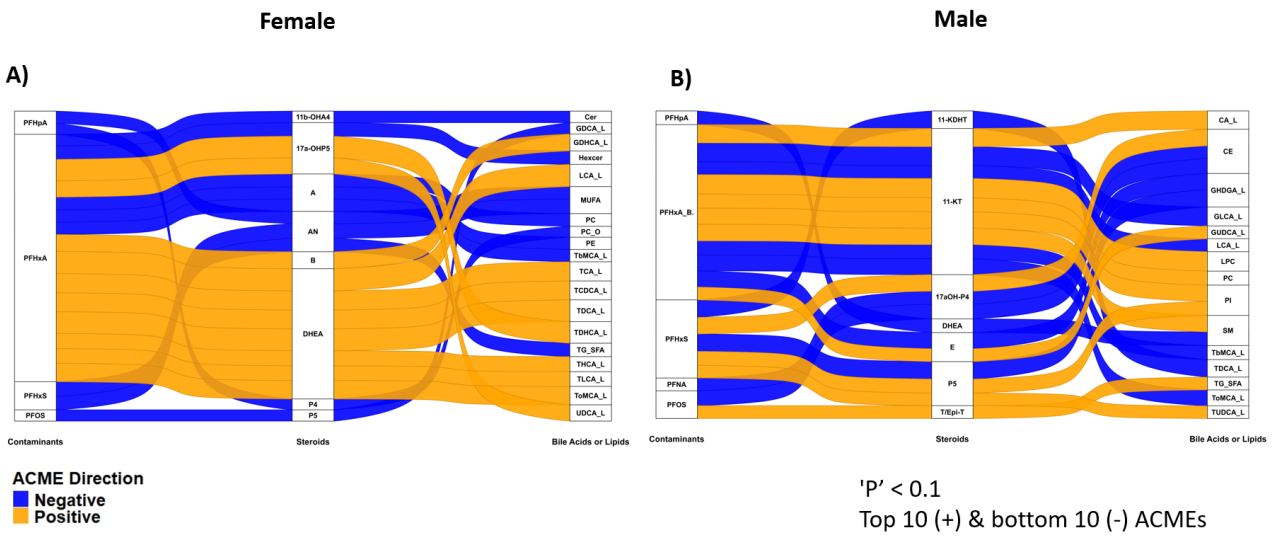

Fig. S14. The causal mediation analysis results showing the indirectly mediated effects with (A) female and (B) male subjects.

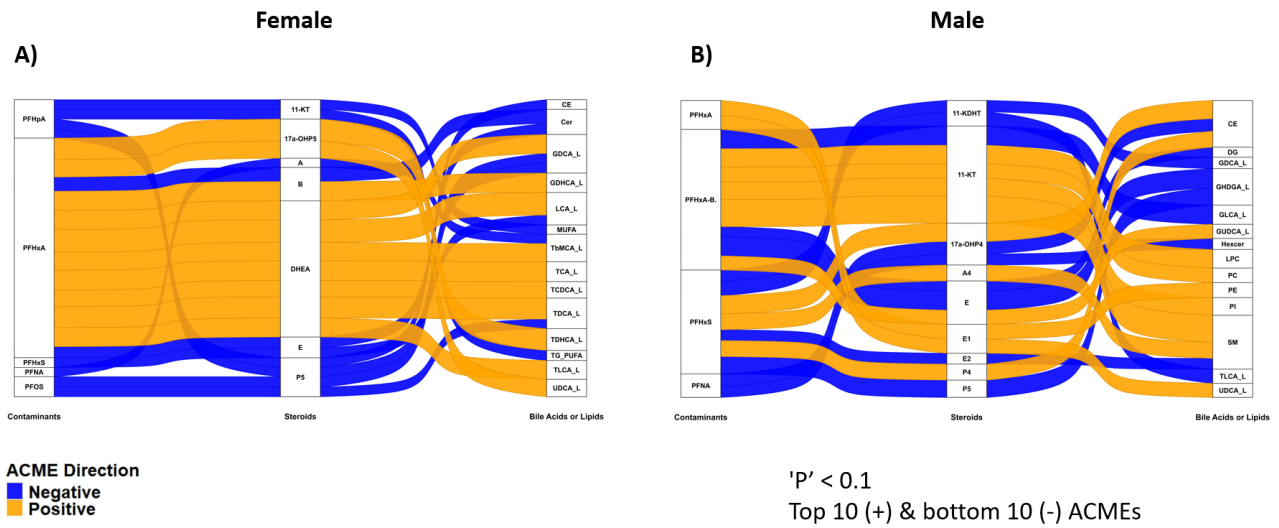

ACME Direction
Negative
Positive

'P' < 0.1
Top 10 (+) & bottom 10 (-) ACMEs

Fig. S15. The causal mediation analysis results showing the indirectly mediated effects with (A) female and (B) male subjects after basic adjustments (age and gender) of the models (Y and M).

Supplementary tables

Table S1. Demographic characteristics of the study population (median, range), divided into three groups (all, females and males).

Median (Q1, Q3) (or min and max)	All Subjects	Female Subjects	Male Subjects
N	104	69	35
Age	49.0 (43.0, 54.3)	46.0 (43.0, 53.0)	52.0 (44.5, 58.0)
BMI	45.3 (41.1, 49.1)	45.11 (41.1, 48.7)	46.3 (41.3, 49.6)
PFAS	0.41 (0.28, 0.57)	0.35 (0.25, 0.53)	0.48 (0.41, 0.70)
HDL	1.1 (1.0, 1.3)	1.1 (1.0, 1.4)	1.0 (0.9, 1.2)
HOMA-IR	3.1 (1.8, 4.6)	3.0 (1.6, 3.9)	3.9 (2.3, 5.4)
Steatosis Grade (min, max)	(0, 3)	(0, 3)	(0, 1)
Fibrosis Stage (min, max)	(0, 4)	(0, 3)	(0, 4)
Necroinflammation (min, max)	(0, 2)	(0, 1)	(0, 2)
HOMA-IR (min, max)	(0.2, 14.5)	(0.2, 14.5)	(0.2, 14.5)

Table S2. The internal standard mix prepared in 30% acetonitrile/70% water with following concentrations.

Compound	Concentration (nM)
d3-17a-OH-Pregnenolone (d3-17a-OHP5)	20
d4-Pregnenolone (d4-P5)	200
d7-11-Deoxycortisol (d7-S)	20
d7-11-Deoxycorticosterone (d7-DOC)	20
d4-Cortisol (d4-F)	20
d9-Progesterone (d9-P4)	20
d8-Cortisone (d8-E)	20
d8-17a-OH-Progesterone (d8-17aOH-P4)	20
d4-Estradiol (d4-E2)	20
d4-Estrone (d4-E1)	20
d4-Androsterone (d4-AN)	20
d3-Testosterone (d3- T/Epi-T)	4
d8-Aldosterone (d8-A)	20
d3-11-Ketotestosterone (d3-11-KT)	20
d3-11-Ketodihydrotestosterone (d3-11-KDHT)	20
d4-11b-OH-Androstenedione (d4-11b-OHA4)	20
d4-Dihydrotestosterone (d4-DHT)	20
d2-Dehydroepiandrosterone (d2-DHEA)	200
d3-Androstenedione (d3-A4)	2

Table S3. Calibration curve levels.

Level	Working solution, nM	Reconstituted LC-MS/MS sample (100 µL), pM	Calibration points conc. pM
U1	0.005	2	1.00
U2	0.01	4	2.00
L1	0.025	10	5.00
L2	0.05	20	10.00
L3	0.1	40	20.00
L4	0.25	100	50.00
L5	0.5	200	100.00
L6	1	400	200.00
L7	2.5	1000	500.00
L8	5	2000	1000.00
L9	10	4000	2000.00
L10	50	20000	10000.00
L11	100	40000	20000.00
L12	250	100000	50000.00
L13	500	200000	100000.00
L14	1000	400000	200000.00

Table S4. UHPLC-MS/MS conditions for steroid analysis.

Liquid chromatography conditions				
Phase A	0.2 mM NH_4F in water			
Phase B	0.2 mM NH_4F in water/methanol (5/95)			
chromatographic column	Kinetex 1.7 um Biphenyl 100 A LC Column 100 x 2.1 mm (00D-4628-AN)			
Gradient	time, min	Flow rate, µL/min	%A	%B
	0.0	300	60	40
	3.5	300	32	68
	9.5	300	29	71
	13.5	300	20	80
	14.5	300	0	100
	19.0	300	0	100
	19.1	300	60	40
	21.0	300	60	40
Column temperature	35ºC			
Autosampler temperature	10ºC			
Injection volume	10 µL			
Analysis time	21 min			
Source parameters				
Ion source			OptiFlow Pro	
Ionization mode			Positive+Negative	
Source temperature, ºC			400	
Spray voltage, V			1500	
Ion source gas 1, psi			40	
Ion source gas 2, psi			70	
Entrance potential (EP), V			-10/10	

MS/MS transitions conditions										
Group	Compound ID	RT, min	RT window, (+/- s)	Q1	Q2	Dwell time, ms	CE, V	CXP, V	Q0	ionization mode
F	d4-F	5.6	50	367.25	121.1	81.5	29	16	-10	pos
F	F 1	5.6	50	363.1	121.2	81.5	31	8	-10	pos
F	F 2	5.6	50	363.1	91	81.5	83	10	-10	pos
E	d8-E	6.25	50	369.23	169	39.3	33	20	-10	pos

E	E 1	6.25	50	361.1	163.1	39.3	31	26	-10	pos
E	E 2	6.25	50	361.1	77	39.3	107	10	-10	pos
11-KT	d3-11-KT	7.7	50	306.24	262.187	35.5	31	26	-10	pos
11-KT	11-KT 1	7.7	50	303.4	259.168	35.5	31	26	-10	pos
11-KT	11-KT 2	7.7	50	303.4	121.027	35.5	31	0	-10	pos
17a-OHP5	d3-17a-OHP5	7.2	50	336.24	300.246	31.4	15	17	10	pos
17a-OHP5	17a-OHP5 1	7.2	50	333.11	297.1	31.4	13	22	10	pos
17a-OHP5	17a-OHP5 2	7.2	50	333.48	315.06	31.4	10	18	10	pos
S	d7-S	8.9	50	354.05	100.077	3.0	33	16	-10	pos
S	S 1	9	50	347.06	97	3.0	27	12	-10	pos
S	S 2	9	50	347.06	109	3.0	33	16	-10	pos
B	d8-B	9.5	90	355.46	337	31.4	32	11	-10	pos
B	B1	9.5	90	347.46	329.18	31.4	21	22	-10	pos
B	B2	9.5	90	347.1	121.1	31.4	29	8	-10	pos
11b-OHA4	d4-11b-OHA4	9.15	50	307.3	270.256	25.0	25	15	-10	pos
11b-OHA4	11b-OHA4 1	9.15	50	303.2	267.175	25.0	24	14	-10	pos
11b-OHA4	11b-OHA4 2	9.15	50	303.2	285.189	25.0	22	16	-10	pos
11-KDHT	d3-11-KDHT	9.2	50	308.4	254.231	24.5	25	24	50	pos
11-KDHT	11-KDHT 1	9.2	50	305.4	251.164	24.5	25	21	50	pos
11-KDHT	11-KDHT 2	9.2	50	305.4	287.232	24.5	23	20	50	pos
11-KA4	11-KA4 1	9.3	50	301.2	257.14	24.4	31	17	-10	pos
11-KA4	11-KA4 2	9.3	50	301.2	121.04	24.4	31	15	-10	pos
DHEA	DHEA 1	10.5	50	289.08	253	31.5	15	46	30	pos
DHEA	DHEA 2	10.5	50	289.4	271.07	31.5	11	28	30	pos
DHEA	d2-DHEA 1	10.5	50	291.2	255.215	31.5	16	14	30	pos
DHEA	d2-DHEA 2	10.5	50	291.2	273.24	31.5	12	15	30	pos
T/Epi-T	d3-T	11.87	50	292.06	97	36.8	29	12	-10	pos
T/Epi-T	T/Epi-T 1	11.87	50	289.06	97	36.8	29	12	-10	pos
T/Epi-T	T/Epi-T 2	11.87	50	289.06	109.2	36.8	31	6	-10	pos

17aOH-P4	d8-17aOH-P4	11.6	50	339.05	100.077	37.4	27	12	-10	pos
17aOH-P4	17aOH-P4 1	11.7	50	331.05	109.1	36.6	31	12	-10	pos
17aOH-P4	17aOH-P4 2	11.7	50	331.05	96.9	36.6	29	12	-10	pos
AN	d4-AN	12.1	60	277.2	259.241	42.3	19	25	-10	pos
AN	AN 1	12.1	60	273	255	42.3	20	12	-10	pos
AN	AN 2	12.1	60	273	147	42.3	30	14	-10	pos
DHT	d4-DHT	13	60	295.2	259.221	64.2	23	14	10	pos
DHT	DHT 1	13.1	60	291.29	255.2	65.9	21	30	10	pos
DHT	DHT 2	13.1	60	291.44	273.03	65.9	10	18	10	pos
A4	d3-A4 1	14.55	50	290.2	109.063	5.0	32	14	-10	pos
A4	d3-A4 2	14.55	50	290.2	100.08	5.0	29	16	-10	pos
A4	A4 1	14.55	50	287.04	97	5.0	27	14	-10	pos
A4	A4 2	14.55	50	287.04	78.9	5.0	67	10	-10	pos
DOC	d7-DOC 1	15	50	338.2	100.071	56.7	28	11	-10	pos
DOC	d7-DOC 2	15	50	338.2	112.025	56.7	31	20	-10	pos
DOC	DOC 1	15	50	331.2	97	56.7	29	16	-10	pos
DOC	DOC 2	15	50	331.2	109	56.7	31	12	-10	pos
P5	d4-P5	14.25	50	321.1	285.1	58.8	20	16	-10	pos
P5	P5 1	14.25	50	317.48	299.13	58.8	15	16	-10	pos
P5	P5 2	14.25	50	317.1	281.1	58.8	17	16	-10	pos
P4	d9-P4	16.15	50	324	113	105.1	23	10	-10	pos
P4	P4 1	16.15	50	315.06	97.1	105.1	23	10	-10	pos
P4	P4 2	16.15	50	315.06	109.1	105.1	27	10	-10	pos
A	d8-A	7.3	50	367.174	193.9	31.8	-26	-21	10	neg
A	A 1	7.3	50	359.093	189.1	31.8	-26	-21	10	neg
A	A 2	7.3	50	359.093	331	31.8	-22	-35	10	neg
E2	d4-E2	6.6	50	275	147.8	31.7	-55	-22	10	neg
E2	E2 1	6.6	50	271	182.9	31.7	-52	-19	10	neg
E2	E2 2	6.6	50	271	144.9	31.7	-60	-21	10	neg
E1	d4-E1	9.85	50	273	147	25.5	-60	-20	10	neg

E1	E1 1	9.85	50	269.1	144.9	25.5	-48	-15	10	neg
E1	E1 2	9.85	50	269.1	142.9	25.5	-70	-15	10	neg

Table S5. Instrumentation.

Instrument Model	Serial Number
ExionLC AD Pump	AB3AD5976127
ExionLC AD Pump	AB3AD5976128
ExionLC AD Autosampler	AB3AC5972305
AC Column Oven	AB2CT5972057
System Controller	ABCBM5974024
SCIEX Triple Quad™ 7500	FA220602109

Table S6. The medians of steroid concentrations (pM) with interquartile ranges (Q1 and Q3).

Steroid Name	Abbreviation of Steroid	Steroid Category	Median (Q1, Q3) (pM)	Median (Q1, Q3) (pM)	Median (Q1, Q3) (pM)
11-Ketotestosterone	11-KT	Androgens	926 (617, 1161)	925 (606, 1163)	942 (759, 1087)
11b-OH-Androstenedione	11b-OHA4	Androgens	8870 (6700, 11868)	9461 (6379, 11406)	8663 (7510, 12528)
11-Ketodihydrotestosterone	11-KDHT	Androgens	100 (100, 100)	100 (100, 100)	100 (100, 153)
11-Ketoandrostenedione	11-KA4	Androgens	1262 (845, 1687)	1262 (838, 1663)	1318 (890, 1699)
Dehydroepiandrosterone	DHEA	Androgens	8294 (5602, 12330)	9395 (6072, 13100)	6683 (5301, 9524)
Testosterone / Epi-testosterone	T/Epi-T	Androgens	1225 (838, 8089)	913 (717, 1216)	10808 (8204, 13367)
Androsterone	AN	Androgens	250 (250, 507)	250 (250, 505)	250 (250, 410)
Dihydrotestosterone	DHT	Androgens	276 (132, 461)	203 (109, 311)	524 (381, 632)
Androstenedione	A4	Androgens	2226 (1548, 3064)	2366 (1578, 3276)	1995 (1539, 2424)
Estradiol	E2	Estrogens	137 (77, 271)	167 (66, 441)	117 (104, 175)
Estrone	E1	Estrogens	271 (170, 407)	321 (193, 482)	232 (166, 285)
Cortisone	E	Glucocorticoids	40685 (33628, 45755)	40538 (30857, 45250)	42424 (37906, 49608)
11-Deoxycortisol	S	Glucocorticoids	843 (560, 1134)	810 (533, 1050)	892 (576, 1346)
Corticosterone	B	Mineralocorticoids	7258 (5046, 12538)	7545 (5054, 12526)	6495 (5085, 12852)
Aldosterone	A	Mineralocorticoids	1105 (685, 1827)	1291 (925, 2004)	722 (443, 1142)
11-Deoxycorticosterone	DOC	Mineralocorticoids	62 (47, 90)	60 (48, 96)	67 (44, 87)
17a-OH-Pregnenolone	17a-OHP5	Progestogens	1613 (924, 3290)	1615 (776, 3293)	1612 (1190, 3050)
17a-OH-Progesterone	17a-OHP4	Progestogens	1121 (631, 1717)	830 (527, 1510)	1510 (1076, 1839)
Pregnenolone	P5	Progestogens	2091 (1288, 4116)	2375 (1370, 4172)	1584 (1120, 2464)
Progesterone	P4	Progestogens	124 (79, 262)	160 (92, 586)	94 (75, 146)

Table S7. The medians of PFAS, bile acid and lipid concentrations (pM) with interquartile ranges (Q1 and Q3).

	All	Female	Male
Compounds	Median (Q1, Q3) (pM)	Median (Q1, Q3) (pM)	Median (Q1, Q3) (pM)
PFHpA	0.05 (0.04, 0.08)	0.05 (0.03, 0.07)	0.08 (0.06, 0.09)
PFHxA	0.21 (0.18, 0.25)	0.20 (0.18, 0.25)	0.23 (0.18, 0.26)
PFHxA_Branched	2.47 (1.55, 5.48)	2.45 (1.50, 4.59)	2.77 (1.67, 7.06)
PFHxS	0.04 (0.03, 0.05)	0.03 (0.03, 0.05)	0.05 (0.04, 0.07)
PFNA	0.03 (0.02, 0.03)	0.02 (0.02, 0.03)	0.03 (0.02, 0.04)
PFOA	0.13 (0.09, 0.16)	0.13 (0.08, 0.16)	0.13 (0.10, 0.17)
PFOS	0.14 (0.10, 0.24)	0.12 (0.09, 0.21)	0.18 (0.15, 0.27)
CA	11 (7, 16)	11 (7, 16)	11 (7, 16)
CDCA	31 (27, 37)	31 (27, 37)	30 (28, 43)
DCA	21 (17, 26)	22 (18, 26)	19 (16, 26)
LCA	94 (84, 100)	95 (85, 100)	90 (84, 102)
UDCA	7 (5, 11)	9 (6, 13)	7 (4, 8)
GCA	15967 (9475, 23383)	17187 (9272, 23102)	14579 (10409, 22390)
GCDCA	14801 (8961, 23899)	15554 (8549, 24877)	12739 (9313, 21418)
GDCA	7438 (3298, 14389)	7835 (4314, 15531)	5828 (1410, 12555)
GDHCA	2 (2, 3)	2 (2, 3)	2 (2, 3)
GHCA	22 (12, 38)	25 (14, 40)	19 (10, 30)
GHDGA	3 (0, 7)	3 (0, 6)	3 (0, 8)
GLCA	341 (182, 607)	354 (214, 590)	310 (157, 656)

GUDCA	1184 (565, 2334)	1238 (588, 2503)	962 (546, 1773)
TbMCA	29 (11, 81)	33 (13, 80)	26 (11, 80)
ToMCA	17 (14, 25)	18 (14, 25)	17 (12, 24)
TCA	4700 (3054, 6914)	4387 (2831, 6474)	6000 (3680, 7981)
TCDCA	4950 (3174, 7237)	4772 (2966, 7203)	5351 (3712, 7027)
TDCA	1559 (857, 3996)	1696 (875, 3897)	1423 (629, 4361)
TDHCA	11 (10, 14)	11 (10, 14)	12 (10, 14)
THCA	18 (15, 24)	18 (15, 24)	17 (15, 21)
TLCA	127 (67, 244)	135 (70, 250)	124 (63, 240)
TUDCA	116 (73, 214)	112 (71, 215)	118 (79, 214)
C4	35 (19, 66)	35 (21, 70)	33 (17, 48)
Cer	33 (28, 38)	33 (28, 38)	32 (29, 39)
CE	4 (4, 5)	4 (4, 5)	4 (3, 4)
DG	7 (5, 9)	7 (5, 9)	7 (6, 9)
Hexcer	7 (6, 8)	7 (6, 8)	8 (6, 9)
LPC	6 (5, 7)	6 (5, 7)	7 (5, 8)
PC	82 (72, 89)	83 (72, 89)	82 (75, 87)
PC_O	6 (5, 7)	6 (5, 6)	7 (6, 8)
PE	48 (44, 51)	46 (43, 50)	49 (47, 53)
PI	7 (6, 8)	7 (6, 8)	7 (6, 8)
SM	20 (18, 23)	19 (18, 22)	22 (19, 25)
TG_SFA	53 (36, 82)	57 (37, 79)	47 (36, 88)
MUFA	36 (23, 51)	34 (21, 50)	43 (30, 57)
TG_PUFA	31 (23, 46)	28 (21, 40)	33 (25, 51)

Table S8. Top 20 unadjusted mediation analysis results as per descending indirect effect (ACME) order of magnitude using all subjects. The calculation for the link was done assuming that mediation happens in the liver. Liver bile acids were also in serum, hence the '_L' at the end to differentiate. Definitions: ADE = average direct effects, the p values, d0.p for ACME and similarly for others (ADE, proportion mediated and total effect), are fraction of simulations that are above or below zero, where the lowest one is selected and multiplied with two, and ci_l=lower confidence interval and ci_u=upper confidence interval.

Mediation 'Link': Contaminant -> Steroid -> Bile Acid / Lipid	ACME	d0.p	d0.ci_l	d0.ci_u	ADE	z0.p	z0.ci_l	z0.ci_u	Proportion Mediated	n1.p	n.ci_l	n1.ci_u	Total Effect	tau.p	tau.ci_l	tau.ci_u
PFHxS T/Epi-T PC_O	0.78	0.00	0.23	1.41	1.04	0.06	-0.14	1.98	0.40	0.02	0.12	0.97	1.82	0.02	0.63	2.96
PFHxS T/Epi-T PE	0.68	0.00	0.15	1.43	-0.76	0.34	-2.14	0.63	-0.07	1.00	-18.78	14.38	-0.08	1.00	-1.33	1.04
PFHxS T/Epi-T SM	0.61	0.02	0.15	1.37	-0.85	0.24	-1.95	0.34	-0.60	0.68	-11.94	14.35	-0.24	0.70	-1.31	0.94
PFHxS T/Epi-T TG_PUFA	0.59	0.02	0.02	1.30	-0.90	0.28	-2.24	0.74	-0.38	0.62	-8.29	6.28	-0.31	0.64	-1.89	1.32
PFHxS E2 LCA_L	0.56	0.00	0.11	1.10	-1.12	0.14	-2.73	0.23	-0.56	0.44	-5.38	12.43	-0.56	0.44	-1.83	0.80
PFHpA T/Epi-T SM	0.55	0.00	0.14	1.01	-1.18	0.00	-2.09	-0.50	-0.78	0.10	-7.15	5.91	-0.63	0.10	-1.48	0.10
PFHxA 17a-OHP5 PE	0.54	0.00	0.09	1.16	0.79	0.44	-1.14	2.28	0.33	0.16	-5.36	2.79	1.33	0.16	-0.47	2.93
PFHpA T/Epi-T PE	0.54	0.00	0.11	0.96	-1.01	0.00	-1.92	-0.21	-0.86	0.26	-6.27	7.82	-0.47	0.26	-1.34	0.33
PFHxA DHEA PC	0.52	0.04	0.02	1.11	-0.74	0.40	-2.26	1.07	-0.24	0.80	-4.79	12.78	-0.22	0.76	-1.80	1.51
PFHxA DHT PC_O	0.51	0.06	-0.06	1.27	0.87	0.24	-0.73	2.17	0.35	0.12	-0.42	3.15	1.38	0.06	-0.02	2.62
PFHxA 17a-OHP5 UDCA_L	0.51	0.04	0.02	1.09	-1.26	0.14	-2.76	0.43	-0.35	0.44	-3.20	5.05	-0.75	0.40	-2.14	0.73
PFHpA T/Epi-T PC_O	0.49	0.00	0.19	0.78	0.57	0.16	-0.24	1.25	0.46	0.00	0.17	2.10	1.05	0.00	0.16	1.78
PFHxS T/Epi-T LPC	0.48	0.10	-0.05	1.07	-1.24	0.06	-2.59	0.07	-0.33	0.42	-6.32	12.41	-0.76	0.32	-2.01	0.55
PFHxA 17a-OHP5 PI	0.48	0.04	0.04	1.22	-0.10	0.80	-1.48	1.61	0.45	0.58	-12.47	8.90	0.38	0.58	-1.00	1.91
PFHxA E LCA_L	0.48	0.08	-0.04	1.20	0.40	0.62	-1.21	2.01	0.36	0.36	-2.86	4.67	0.88	0.28	-0.90	2.53
PFHxS T/Epi-T CDCA_L	0.46	0.12	-0.16	1.09	-1.26	0.08	-2.90	0.25	-0.31	0.48	-8.69	6.06	-0.79	0.36	-2.59	0.66

PFHxA DHEA PI	0.46	0.06	0.01	1.14	-0.11	0.82	-1.38	1.78	0.19	0.82	-9.46	6.86	0.35	0.76	-1.03	2.13
PFHxA 17a-OHP5 TDHCA_L	0.46	0.02	0.03	1.04	-0.22	0.76	-1.68	1.86	0.16	0.90	-16.48	10.94	0.24	0.88	-1.11	2.24
PFHxA DHEA TCA_L	0.46	0.08	-0.02	1.14	-0.12	0.82	-1.50	1.27	0.42	0.66	-4.52	10.36	0.33	0.62	-1.14	1.71
PFOS T/Epi-T PC_O	0.45	0.00	0.10	0.91	0.17	0.80	-0.52	1.03	0.72	0.10	-3.36	6.19	0.62	0.10	-0.06	1.52

Table S9. Top 20 unadjusted mediation analysis results as per descending indirect effect (ACME) order of magnitude using female subjects. The calculation for the link was done assuming that mediation happens in the liver. Liver bile acids were also in serum, hence the '_L' at the end to differentiate. Definitions: ADE = average direct effects, the p values, d0.p for ACME and similarly for others (ADE, proportion mediated and total effect), are fraction of simulations that are above or below zero, where the lowest one is selected and multiplied with two, and ci_l=lower confidence interval and ci_u=upper confidence interval.

Mediation 'Link': Contaminant -> Steroid -> Bile Acid / Lipid	ACME	d0.p	d0.ci_l	d0.ci_u	ADE	z0.p	z0.ci_l	z0.ci_u	Proportion Mediated	n1.p	n.ci_l	n1.ci_u	Total Effect	tau.p	tau.ci_l	tau.ci_u
PFHxA DHEA LCA_L	0.86	0.02	0.25	1.77	0.04	0.96	-1.56	1.48	0.84	0.22	-5.62	19.73	0.91	0.20	-0.55	2.55
PFHxA DHEA TDCA_L	0.85	0.04	0.07	1.78	-0.79	0.42	-2.58	1.01	0.03	1.00	-20.23	6.04	0.06	0.96	-1.78	1.55
PFHxA 17a-OHP5 TDHCA_L	0.84	0.00	0.27	1.52	0.08	0.84	-1.80	1.86	0.62	0.28	-4.58	7.61	0.92	0.28	-1.04	2.71
PFHxA DHEA TCA_L	0.75	0.00	0.15	1.79	-0.44	0.60	-2.36	1.68	0.28	0.86	-14.60	22.70	0.31	0.86	-1.45	2.51
PFHxA DHEA TCDCA_L	0.74	0.04	0.09	1.75	-0.47	0.66	-2.70	1.19	0.46	0.72	-7.41	8.38	0.27	0.68	-1.49	1.84
PFHxA DHEA ToMCA_L	0.72	0.08	-0.06	1.47	-0.29	0.78	-2.20	1.56	0.45	0.66	-5.35	10.35	0.43	0.62	-1.39	2.22
PFHxA B GDHCA_L	0.66	0.02	0.02	1.48	-0.98	0.24	-2.49	0.76	-0.46	0.64	-27.91	7.60	-0.32	0.62	-1.79	1.51
PFHxA DHEA GDCA_L	0.64	0.10	-0.05	1.96	-0.59	0.54	-2.21	1.51	-0.09	0.94	-8.06	7.16	0.05	0.92	-1.86	2.09
PFHxA 17a-OHP5 UDCA_L	0.63	0.04	0.01	1.54	-0.47	0.50	-2.05	1.25	0.17	0.90	-13.09	29.91	0.17	0.90	-1.49	1.52
PFHxA DHEA THCA_L	0.59	0.08	-0.03	1.40	-0.32	0.70	-2.05	1.78	0.34	0.78	-4.47	6.73	0.27	0.78	-1.60	2.26
PFHxA DHEA TLCA_L	0.57	0.06	0.01	1.37	-1.01	0.20	-2.39	0.49	-0.39	0.64	-13.40	8.62	-0.44	0.58	-1.87	1.00
PFHxA E LCA_L	0.56	0.02	0.05	1.37	0.53	0.64	-1.72	2.17	0.34	0.24	-0.83	8.90	1.08	0.22	-1.03	2.82
PFHxS E2 LCA_L	0.51	0.00	0.13	1.10	-0.25	0.58	-1.22	0.76	0.63	0.68	-5.45	7.31	0.26	0.68	-0.78	1.40
PFHxA E GDHCA_L	0.50	0.14	-0.06	1.44	-1.01	0.40	-2.92	1.18	-0.18	0.66	-4.29	10.63	-0.51	0.68	-2.34	1.40
PFHxA B GLCA_L	0.50	0.08	0.00	1.32	0.69	0.52	-1.12	2.36	0.29	0.24	-1.38	3.34	1.19	0.16	-0.53	2.95
PFHxA 17a-OHP5 LCA_L	0.50	0.22	-0.43	1.32	0.58	0.52	-1.19	2.63	0.33	0.44	-1.30	2.17	1.08	0.26	-0.76	3.05
PFHxA 11b-OHA4 TG_PUFA	0.48	0.06	-0.01	1.14	-0.53	0.56	-2.27	1.16	-0.09	0.88	-18.04	5.37	-0.05	0.90	-1.85	1.59
PFHxA DHEA GLCA_L	0.48	0.16	-0.15	1.35	0.57	0.52	-1.22	2.30	0.29	0.44	-7.12	4.57	1.04	0.28	-0.59	2.73
PFHxA 17a-OHP5 GHDGA_L	0.46	0.16	-0.08	1.32	-2.48	0.00	-4.13	-0.81	-0.21	0.16	-0.96	0.04	-2.03	0.00	-3.64	-0.60
PFHxA DHEA TbMCA_L	0.45	0.26	-0.24	1.57	-0.67	0.48	-2.54	1.11	-0.22	0.80	-5.85	35.43	-0.22	0.82	-1.94	1.57

Table S10. Top 20 unadjusted mediation analysis results as per descending indirect effect (ACME) order of magnitude using male subjects. The calculation for the link was done assuming that mediation happens in the liver. Liver bile acids were also in serum, hence the '_L' at the end to differentiate. Definitions: ADE = average direct effects, the p values, d0.p for ACME and similarly for others (ADE, proportion mediated and total effect), are fraction of simulations that are above or below zero, where the lowest one is selected and multiplied with two, and ci_l=lower confidence interval and ci_u=upper confidence interval.

Mediation 'Link': Contaminant -> Steroid -> Bile Acid / Lipid	ACME	d0.p	d0.ci_l	d0.ci_u	ADE	z0.p	z0.ci_l	z0.ci_u	Proportion Mediated	n1.p	n.ci_l	n1.ci_u	Total Effect	tau.p	tau.ci_l	tau.ci_u
PFHxA_Branched 11-KT LPC	0.85	0.04	0.20	1.77	-1.02	0.10	-2.41	0.20	-0.49	0.84	-14.70	11.23	-0.17	0.80	-1.67	1.06
PFHxA_Branched 11-KT CA_L	0.80	0.02	0.10	1.61	-1.54	0.04	-3.08	-0.14	-0.79	0.30	-22.21	17.06	-0.74	0.28	-2.39	0.54
PFHxS 17aOH-P4 CE	0.73	0.02	0.03	1.86	0.60	0.58	-1.11	2.60	0.48	0.22	-2.20	2.88	1.33	0.20	-0.52	3.19
PFHxA_Branched 11-KT SM	0.73	0.06	-0.03	1.48	-0.42	0.46	-1.94	1.17	0.82	0.66	-7.46	15.85	0.30	0.64	-0.91	1.82
PFHxA_Branched 11-KT PI	0.71	0.04	0.04	1.65	-0.08	0.84	-1.38	1.19	0.78	0.36	-5.35	12.14	0.63	0.32	-0.65	1.89
PFHxS 17aOH-P4 SM	0.67	0.10	-0.09	1.73	-0.75	0.36	-2.23	0.88	-0.21	0.88	-15.97	9.12	-0.08	0.94	-1.49	1.66
PFNA 11-KT PI	0.63	0.10	-0.09	1.77	-0.73	0.22	-1.67	0.62	-0.04	0.98	-28.17	16.49	-0.10	0.88	-1.52	1.29
PFHxA_Branched 11-KT PC	0.62	0.04	0.04	1.47	0.07	0.90	-1.31	1.47	0.50	0.36	-8.02	7.91	0.69	0.36	-0.58	2.06
PFHxS P5 PI	0.61	0.06	-0.01	1.62	-1.30	0.16	-2.96	0.41	-0.39	0.46	-5.42	4.70	-0.68	0.40	-2.36	1.27
PFNA 11-KT LPC	0.57	0.12	-0.06	1.63	-0.85	0.28	-2.90	0.66	-0.25	0.74	-14.37	8.34	-0.28	0.74	-1.83	1.17
PFOA P5 GHDGA_L	0.57	0.14	-0.26	1.36	0.12	0.90	-1.60	1.62	0.39	0.42	-7.34	8.57	0.69	0.44	-0.98	2.39
PFHxS P5 PC	0.57	0.10	-0.09	1.42	-1.16	0.26	-2.63	0.39	-0.39	0.52	-8.19	9.23	-0.59	0.42	-2.18	0.82
PFHxA_Branched E GUDCA_L	0.57	0.04	0.05	1.41	-1.17	0.10	-2.37	0.20	-0.61	0.32	-31.34	3.99	-0.60	0.28	-1.77	0.43
PFOS T/Epi-T TG_SFA	0.56	0.06	0.00	1.35	-1.21	0.16	-2.47	0.39	-0.41	0.44	-7.66	4.03	-0.64	0.38	-1.95	1.00
PFHxS P5 TUDCA_L	0.55	0.06	0.02	1.38	-0.92	0.22	-2.20	0.52	-0.30	0.66	-11.62	8.53	-0.37	0.60	-1.67	1.24
PFNA 11-KT PC	0.55	0.08	-0.14	1.17	-0.76	0.30	-2.01	0.51	-0.26	0.88	-20.19	10.70	-0.21	0.80	-1.68	1.42
PFNA 11-KT SM	0.54	0.08	-0.03	1.30	-0.92	0.18	-2.46	0.37	-0.35	0.70	-10.15	6.61	-0.38	0.62	-2.33	0.86
PFHxS 17aOH-P4 Hexcer	0.54	0.18	-0.25	1.56	-0.35	0.72	-2.25	1.30	0.16	0.88	-5.72	8.36	0.19	0.82	-1.78	1.91
PFHxS P5 GUDCA_L	0.54	0.10	-0.08	1.42	-1.71	0.02	-3.20	-0.12	-0.37	0.18	-9.11	1.33	-1.18	0.12	-2.86	0.35
PFHxS A4 SM	0.53	0.20	-0.22	1.90	-0.53	0.54	-2.17	1.04	0.23	0.86	-5.16	6.43	0.00	0.98	-1.68	2.11

Table S11. Maaslin-2 linear model results for steroids in cases here in order fibrosis, HOMA-IR, necroinflammation and steatosis.

Steroid	Gender in Condition	Coef	Stderr	Pval	Qval	N	N Not Zero	Steroid	Gender in Condition	Coef	Stderr	Pval	Qval	N	N Not Zero
DHT	Fibrosis_both	-0.245	0.085	0.005	0.037	104	58	DHT	Necroinflammation_both	-0.244	0.084	0.004	0.035	104	58
11-KA4	Fibrosis_both	0.169	0.100	0.093	0.353	104	94	DOC	Necroinflammation_both	-0.263	0.098	0.008	0.056	104	52
AN	Fibrosis_both	-0.156	0.094	0.101	0.353	104	27	AN	Necroinflammation_both	-0.208	0.092	0.026	0.129	104	27
P5	Fibrosis_both	-0.155	0.099	0.123	0.392	104	50	B	Necroinflammation_both	-0.215	0.099	0.032	0.151	104	48
T/Epi-T	Fibrosis_both	-0.056	0.042	0.193	0.483	104	40	P5	Necroinflammation_both	-0.209	0.097	0.034	0.151	104	50
S	Fibrosis_both	-0.120	0.099	0.228	0.507	104	54	P4	Necroinflammation_both	-0.173	0.087	0.049	0.196	104	32
DOC	Fibrosis_both	-0.128	0.102	0.209	0.507	104	52	17a-OHP4	Necroinflammation_both	-0.170	0.095	0.075	0.239	104	55
11-KT	Fibrosis_both	-0.081	0.101	0.428	0.751	104	58	A4	Necroinflammation_both	-0.170	0.094	0.074	0.239	104	56
17a-OHP5	Fibrosis_both	-0.062	0.100	0.535	0.751	104	54	S	Necroinflammation_both	-0.154	0.097	0.117	0.323	104	54
B	Fibrosis_both	-0.073	0.102	0.474	0.751	104	48	E2	Necroinflammation_both	-0.145	0.095	0.129	0.333	104	50
11b-OHA4	Fibrosis_both	0.067	0.099	0.499	0.751	104	58	A	Necroinflammation_both	-0.130	0.092	0.161	0.367	104	56
DHEA	Fibrosis_both	-0.076	0.095	0.424	0.751	104	53	11-KA4	Necroinflammation_both	0.114	0.099	0.255	0.467	104	94
17a-OHP4	Fibrosis_both	-0.063	0.097	0.517	0.751	104	55	E1	Necroinflammation_both	-0.090	0.092	0.330	0.574	104	50
E1	Fibrosis_both	0.055	0.094	0.561	0.774	104	50	E	Necroinflammation_both	-0.073	0.099	0.464	0.646	104	62
E	Fibrosis_both	-0.045	0.100	0.657	0.812	104	62	17a-OHP5	Necroinflammation_both	-0.085	0.099	0.390	0.646	104	54
11-KDHT	Fibrosis_both	-0.042	0.097	0.663	0.812	104	20	T/Epi-T	Necroinflammation_both	-0.036	0.042	0.399	0.646	104	40
A4	Fibrosis_both	-0.041	0.097	0.670	0.812	104	56	11b-OHA4	Necroinflammation_both	0.063	0.098	0.518	0.651	104	58
P4	Fibrosis_both	-0.026	0.089	0.770	0.867	104	32	DHEA	Necroinflammation_both	-0.061	0.094	0.521	0.651	104	53
A	Fibrosis_both	-0.020	0.094	0.832	0.888	104	56	11-KT	Necroinflammation_both	-0.028	0.101	0.779	0.842	104	58
E2	Fibrosis_both	0.020	0.097	0.840	0.888	104	50	11-KDHT	Necroinflammation_both	0.002	0.096	0.980	0.980	104	20
DHT	Fibrosis_female	-0.282	0.106	0.010	0.153	69	27	DHT	Necroinflammation_female	-0.372	0.102	0.001	0.011	69	27
11-KT	Fibrosis_female	-0.208	0.135	0.129	0.554	69	37	DOC	Necroinflammation_female	-0.292	0.124	0.022	0.216	69	33
S	Fibrosis_female	-0.080	0.116	0.493	0.886	69	34	P5	Necroinflammation_female	-0.232	0.123	0.063	0.344	69	38
B	Fibrosis_female	-0.090	0.126	0.476	0.886	69	33	B	Necroinflammation_female	-0.216	0.124	0.086	0.398	69	33
P5	Fibrosis_female	-0.108	0.125	0.390	0.886	69	38	S	Necroinflammation_female	-0.175	0.115	0.131	0.441	69	34
11-KA4	Fibrosis_female	0.066	0.111	0.552	0.898	69	62	17a-OHP4	Necroinflammation_female	-0.203	0.133	0.132	0.441	69	28
E	Fibrosis_female	-0.078	0.141	0.584	0.923	69	36	P4	Necroinflammation_female	-0.202	0.126	0.114	0.441	69	28
DOC	Fibrosis_female	-0.068	0.129	0.601	0.924	69	33	11b-OHA4	Necroinflammation_female	0.185	0.130	0.161	0.442	69	38
AN	Fibrosis_female	-0.053	0.107	0.622	0.933	69	18	11-KDHT	Necroinflammation_female	0.156	0.110	0.162	0.442	69	11

11b-OHA4	Fibrosis_female	0.042	0.132	0.749	0.937	69	38	E2	Necroinflammation_female	-0.199	0.139	0.155	0.442	69	37
11-KDHT	Fibrosis_female	0.052	0.112	0.643	0.937	69	11	A	Necroinflammation_female	-0.144	0.114	0.211	0.508	69	45
T/Epi-T	Fibrosis_female	-0.019	0.056	0.738	0.937	69	5	17a-OHP5	Necroinflammation_female	-0.150	0.133	0.265	0.549	69	36
E1	Fibrosis_female	-0.054	0.131	0.681	0.937	69	40	11-KA4	Necroinflammation_female	0.114	0.110	0.306	0.599	69	62
P4	Fibrosis_female	-0.033	0.128	0.797	0.957	69	28	E1	Necroinflammation_female	-0.134	0.131	0.309	0.599	69	40
17a-OHP5	Fibrosis_female	0.023	0.134	0.863	0.990	69	36	A4	Necroinflammation_female	-0.086	0.129	0.509	0.719	69	42
DHEA	Fibrosis_female	-0.018	0.122	0.881	0.990	69	41	AN	Necroinflammation_female	-0.064	0.107	0.555	0.722	69	18
17a-OHP4	Fibrosis_female	-0.007	0.136	0.958	0.990	69	28	11-KT	Necroinflammation_female	0.061	0.137	0.658	0.775	69	37
A4	Fibrosis_female	0.008	0.129	0.951	0.990	69	42	T/Epi-T	Necroinflammation_female	-0.022	0.056	0.699	0.807	69	5
A	Fibrosis_female	0.011	0.115	0.925	0.990	69	45	E	Necroinflammation_female	-0.046	0.142	0.747	0.831	69	36
E2	Fibrosis_female	-0.026	0.141	0.853	0.990	69	37	DHEA	Necroinflammation_female	-0.020	0.122	0.868	0.883	69	41
E1	Fibrosis_male	0.176	0.100	0.089	0.409	35	10	AN	Necroinflammation_male	-0.370	0.165	0.033	0.177	35	9
T/Epi-T	Fibrosis_male	-0.091	0.056	0.114	0.455	35	35	A4	Necroinflammation_male	-0.291	0.130	0.033	0.177	35	14
DHT	Fibrosis_male	-0.187	0.118	0.123	0.461	35	31	11-KT	Necroinflammation_male	-0.239	0.122	0.059	0.274	35	21
11-KA4	Fibrosis_male	0.309	0.202	0.136	0.480	35	32	B	Necroinflammation_male	-0.291	0.173	0.102	0.394	35	15
AN	Fibrosis_male	-0.248	0.169	0.153	0.509	35	9	11b-OHA4	Necroinflammation_male	-0.201	0.123	0.112	0.394	35	20
DOC	Fibrosis_male	-0.229	0.163	0.170	0.509	35	19	E	Necroinflammation_male	-0.158	0.105	0.142	0.450	35	26
17a-OHP4	Fibrosis_male	-0.130	0.108	0.237	0.568	35	27	DOC	Necroinflammation_male	-0.213	0.167	0.212	0.529	35	19
P5	Fibrosis_male	-0.202	0.166	0.234	0.568	35	12	P5	Necroinflammation_male	-0.217	0.169	0.208	0.529	35	12
E2	Fibrosis_male	0.065	0.054	0.235	0.568	35	13	DHEA	Necroinflammation_male	-0.183	0.150	0.232	0.556	35	12
17a-OHP5	Fibrosis_male	-0.149	0.134	0.276	0.612	35	18	11-KDHT	Necroinflammation_male	-0.226	0.192	0.248	0.573	35	9
S	Fibrosis_male	-0.198	0.182	0.286	0.613	35	20	S	Necroinflammation_male	-0.200	0.185	0.289	0.620	35	20
11-KDHT	Fibrosis_male	-0.175	0.190	0.364	0.675	35	9	P4	Necroinflammation_male	-0.058	0.060	0.340	0.642	35	4
DHEA	Fibrosis_male	-0.137	0.149	0.365	0.675	35	12	17a-OHP4	Necroinflammation_male	-0.094	0.111	0.404	0.663	35	27
11b-OHA4	Fibrosis_male	0.092	0.124	0.465	0.711	35	20	T/Epi-T	Necroinflammation_male	-0.035	0.059	0.554	0.739	35	35
A4	Fibrosis_male	-0.094	0.137	0.499	0.711	35	14	A	Necroinflammation_male	-0.081	0.168	0.633	0.809	35	11
11-KT	Fibrosis_male	0.054	0.127	0.674	0.793	35	21	17a-OHP5	Necroinflammation_male	-0.047	0.139	0.735	0.881	35	18
B	Fibrosis_male	-0.071	0.177	0.690	0.793	35	15	11-KA4	Necroinflammation_male	0.066	0.213	0.757	0.891	35	32
P4	Fibrosis_male	-0.025	0.059	0.674	0.793	35	4	E1	Necroinflammation_male	-0.023	0.107	0.832	0.919	35	10
A	Fibrosis_male	-0.061	0.165	0.714	0.793	35	11	E2	Necroinflammation_male	0.005	0.056	0.935	0.967	35	13
E	Fibrosis_male	-0.018	0.107	0.867	0.915	35	26	DHT	Necroinflammation_male	0.001	0.125	0.993	0.995	35	31
DHT	HOMAIR_both	-0.170	0.087	0.052	0.277	104	58	DHT	Steatosis_both	-0.253	0.083	0.003	0.026	104	58

T/Epi-T	HOMAIR_both	-0.078	0.042	0.069	0.305	104	40	DOC	Steatosis_both	-0.283	0.097	0.004	0.030	104	52
S	HOMAIR_both	0.175	0.098	0.078	0.312	104	54	P5	Steatosis_both	-0.264	0.095	0.007	0.041	104	50
11b-OHA4	HOMAIR_both	0.167	0.098	0.092	0.332	104	58	P4	Steatosis_both	-0.182	0.086	0.036	0.164	104	32
E2	HOMAIR_both	-0.161	0.096	0.095	0.332	104	50	17a-OHP4	Steatosis_both	-0.179	0.094	0.059	0.249	104	55
11-KT	HOMAIR_both	0.151	0.101	0.138	0.382	104	58	11b-OHA4	Steatosis_both	0.164	0.096	0.091	0.303	104	58
AN	HOMAIR_both	-0.137	0.095	0.150	0.397	104	27	11-KA4	Steatosis_both	0.147	0.098	0.137	0.387	104	94
E	HOMAIR_both	0.130	0.100	0.196	0.475	104	62	B	Steatosis_both	-0.145	0.100	0.149	0.396	104	48
A	HOMAIR_both	0.118	0.093	0.211	0.482	104	56	S	Steatosis_both	-0.126	0.097	0.197	0.418	104	54
E1	HOMAIR_both	-0.119	0.093	0.207	0.482	104	50	11-KDHT	Steatosis_both	0.124	0.095	0.195	0.418	104	20
17a-OHP5	HOMAIR_both	-0.105	0.100	0.295	0.569	104	54	E2	Steatosis_both	-0.127	0.094	0.182	0.418	104	50
11-KDHT	HOMAIR_both	0.087	0.097	0.372	0.650	104	20	E1	Steatosis_both	-0.123	0.091	0.180	0.418	104	50
DHEA	HOMAIR_both	-0.062	0.095	0.517	0.738	104	53	A	Steatosis_both	-0.113	0.092	0.222	0.419	104	56
P5	HOMAIR_both	-0.066	0.101	0.512	0.738	104	50	A4	Steatosis_both	-0.104	0.095	0.276	0.490	104	56
17a-OHP4	HOMAIR_both	-0.052	0.097	0.596	0.795	104	55	DHEA	Steatosis_both	-0.086	0.093	0.358	0.607	104	53
DOC	HOMAIR_both	-0.051	0.102	0.622	0.795	104	52	17a-OHP5	Steatosis_both	-0.088	0.098	0.372	0.607	104	54
B	HOMAIR_both	-0.032	0.103	0.753	0.861	104	48	11-KT	Steatosis_both	0.080	0.100	0.425	0.667	104	58
A4	HOMAIR_both	0.007	0.097	0.945	0.996	104	56	T/Epi-T	Steatosis_both	-0.023	0.042	0.579	0.724	104	40
P4	HOMAIR_both	0.003	0.089	0.971	0.996	104	32	AN	Steatosis_both	-0.049	0.094	0.601	0.729	104	27
11-KA4	HOMAIR_both	0.000	0.101	0.998	0.998	104	94	E	Steatosis_both	0.002	0.099	0.982	0.994	104	62
DHT	HOMAIR_female	-0.182	0.108	0.095	0.493	69	27	11-KDHT	Steatosis_female	0.276	0.105	0.011	0.128	69	11
E2	HOMAIR_female	-0.232	0.135	0.090	0.493	69	37	DHT	Steatosis_female	-0.278	0.105	0.010	0.128	69	27
E1	HOMAIR_female	-0.198	0.127	0.124	0.517	69	40	DOC	Steatosis_female	-0.263	0.124	0.037	0.274	69	33
17a-OHP5	HOMAIR_female	-0.152	0.130	0.248	0.577	69	36	11b-OHA4	Steatosis_female	0.240	0.127	0.064	0.318	69	38
B	HOMAIR_female	-0.144	0.123	0.247	0.577	69	33	P5	Steatosis_female	-0.202	0.122	0.103	0.407	69	38
11b-OHA4	HOMAIR_female	0.155	0.129	0.233	0.577	69	38	P4	Steatosis_female	-0.203	0.124	0.108	0.407	69	28
11-KA4	HOMAIR_female	-0.148	0.107	0.174	0.577	69	62	17a-OHP4	Steatosis_female	-0.178	0.132	0.183	0.518	69	28
P5	HOMAIR_female	-0.151	0.122	0.219	0.577	69	38	E1	Steatosis_female	-0.167	0.128	0.198	0.518	69	40
T/Epi-T	HOMAIR_female	-0.062	0.055	0.265	0.582	69	5	11-KT	Steatosis_female	0.147	0.135	0.279	0.559	69	37
11-KDHT	HOMAIR_female	0.109	0.109	0.321	0.630	69	11	11-KA4	Steatosis_female	0.127	0.108	0.247	0.559	69	62
DOC	HOMAIR_female	-0.120	0.126	0.347	0.630	69	33	A	Steatosis_female	-0.128	0.113	0.262	0.559	69	45
DHEA	HOMAIR_female	-0.102	0.119	0.393	0.655	69	41	E2	Steatosis_female	-0.153	0.138	0.270	0.559	69	37
AN	HOMAIR_female	-0.083	0.105	0.430	0.694	69	18	S	Steatosis_female	-0.110	0.115	0.342	0.608	69	34

A	HOMAIR_female	0.085	0.113	0.454	0.698	69	45	B	Steatosis_female	-0.094	0.125	0.452	0.678	69	33
S	HOMAIR_female	0.054	0.114	0.636	0.830	69	34	AN	Steatosis_female	0.055	0.106	0.602	0.786	69	18
11-KT	HOMAIR_female	0.058	0.135	0.667	0.851	69	37	E	Steatosis_female	0.058	0.140	0.680	0.828	69	36
E	HOMAIR_female	0.032	0.139	0.819	0.900	69	36	17a-OHP5	Steatosis_female	-0.042	0.133	0.753	0.828	69	36
17a-OHP4	HOMAIR_female	-0.021	0.133	0.878	0.935	69	28	DHEA	Steatosis_female	0.044	0.120	0.717	0.828	69	41
P4	HOMAIR_female	0.018	0.126	0.888	0.935	69	28	A4	Steatosis_female	-0.015	0.128	0.906	0.955	69	42
A4	HOMAIR_female	-0.013	0.127	0.921	0.953	69	42	T/Epi-T	Steatosis_female	-0.002	0.056	0.978	0.980	69	5
DHT	HOMAIR_male	-0.170	0.087	0.052	0.277	104	58	DHEA	Steatosis_male	-0.448	0.132	0.002	0.038	35	12
T/Epi-T	HOMAIR_male	-0.078	0.042	0.069	0.305	104	40	P5	Steatosis_male	-0.440	0.155	0.008	0.080	35	12
S	HOMAIR_male	0.175	0.098	0.078	0.312	104	54	A4	Steatosis_male	-0.289	0.132	0.036	0.166	35	14
11b-OHA4	HOMAIR_male	0.167	0.098	0.092	0.332	104	58	B	Steatosis_male	-0.341	0.171	0.055	0.221	35	15
E2	HOMAIR_male	-0.161	0.096	0.095	0.332	104	50	DOC	Steatosis_male	-0.318	0.163	0.060	0.224	35	19
11-KT	HOMAIR_male	0.151	0.101	0.138	0.382	104	58	17a-OHP5	Steatosis_male	-0.238	0.133	0.084	0.297	35	18
AN	HOMAIR_male	-0.137	0.095	0.150	0.397	104	27	E	Steatosis_male	-0.174	0.105	0.108	0.340	35	26
E	HOMAIR_male	0.130	0.100	0.196	0.475	104	62	S	Steatosis_male	-0.253	0.185	0.180	0.457	35	20
A	HOMAIR_male	0.118	0.093	0.211	0.482	104	56	11-KT	Steatosis_male	-0.167	0.127	0.197	0.474	35	21
E1	HOMAIR_male	-0.119	0.093	0.207	0.482	104	50	17a-OHP4	Steatosis_male	-0.137	0.110	0.223	0.514	35	27
17a-OHP5	HOMAIR_male	-0.105	0.100	0.295	0.569	104	54	11-KDHT	Steatosis_male	-0.232	0.193	0.238	0.529	35	9
11-KDHT	HOMAIR_male	0.087	0.097	0.372	0.650	104	20	AN	Steatosis_male	-0.191	0.176	0.288	0.616	35	9
DHEA	HOMAIR_male	-0.062	0.095	0.517	0.738	104	53	11b-OHA4	Steatosis_male	-0.115	0.127	0.371	0.666	35	20
P5	HOMAIR_male	-0.066	0.101	0.512	0.738	104	50	P4	Steatosis_male	-0.049	0.060	0.427	0.674	35	4
17a-OHP4	HOMAIR_male	-0.052	0.097	0.596	0.795	104	55	DHT	Steatosis_male	-0.094	0.125	0.455	0.682	35	31
DOC	HOMAIR_male	-0.051	0.102	0.622	0.795	104	52	11-KA4	Steatosis_male	0.139	0.213	0.519	0.692	35	32
B	HOMAIR_male	-0.032	0.103	0.753	0.861	104	48	T/Epi-T	Steatosis_male	-0.040	0.059	0.503	0.692	35	35
A4	HOMAIR_male	0.007	0.097	0.945	0.996	104	56	E2	Steatosis_male	0.019	0.056	0.735	0.852	35	13
P4	HOMAIR_male	0.003	0.089	0.971	0.996	104	32	A	Steatosis_male	-0.038	0.170	0.825	0.884	35	11
11-KA4	HOMAIR_male	0.000	0.101	0.998	0.998	104	94	E1	Steatosis_male	-0.025	0.107	0.817	0.884	35	10